



POTSDAM-INSTITUT FÜR  
KLIMAFOLGENFORSCHUNG

**Originally published as:**

Rezaei, M., [Rousi, E.](#), Ghasemifar, E., Sadeghi, A. (2021): A study of dry spells in Iran based on satellite data and their relationship with ENSO. - Theoretical and Applied Climatology, 144, 3-4, 1387-1405.

**DOI:** [10.1007/s00704-021-03607-y](https://doi.org/10.1007/s00704-021-03607-y)

# A study of dry spells in Iran based on satellite data and their relationship with ENSO

Mohammad Rezaei<sup>1</sup>, Efi Rousi<sup>2</sup>, Elham Ghasemifar<sup>1</sup>, Ali Sadeghi<sup>3</sup>

<sup>1</sup>Department of Climatology, Tarbiat Modares University, Tehran, Iran.

[Mohammad.rezaey@modares.ac.ir](mailto:Mohammad.rezaey@modares.ac.ir)

<sup>2</sup>Potsdam Institute for Climate Impact Research (PIK), Member of the Leibniz Association, Potsdam, Germany.

<sup>3</sup>Department of Geography, Farhangian University, Tehran, Iran.

Corresponding Author: Dr. Mohammad Rezaei

## Abstract

The study of Maximum number of Consecutive Dry Days (MCDDs) is one approach to analyse precipitation behavior in arid and semi-arid regions of Iran. This study is a first attempt to investigate the MCDDs and their relationship with the El Niño/Southern Oscillation (ENSO) in winter months over Iran. The study was carried out using Tropical Rainfall Measuring Mission (TRMM) satellite data on a daily basis at  $1^\circ$  latitude  $\times$   $1^\circ$  longitude spatial resolution and reanalysis data for the period 1998-2019. Results showed that the highest values of MCDDs are observed in southeastern Iran and the lowest in northwestern Iran. Based on the coefficients of the linear trend of the MCDDs, the significant increasing trends are remarkably more abundant than declining trends, especially in the northern half of the country in December and January. The results regarding the relationship between ENSO and MCDDs indicated a non-stationary behavior, with significant negative correlation for December (especially in southwest) and positive correlation for January and February (especially in southeast). The largest differences in the correlation coefficients were observed between December and January. In general, during El Niño (La Niña) phases, the length of MCDDs decreases (increases) in December and increases (decreases) in January especially in the southern half. By comparing different large-scale climate parameters for the two months, we found that during El Niño (La Niña) phases, a negative (positive) anomaly of geopotential height, and a positive (negative) anomaly of zonal wind and specific humidity are observed over the region in December, while the opposite situation occurs in January. The innovation of this study is the use of satellite data that provide a continuous spatial coverage of the region and the consideration of the ENSO teleconnection pattern in regards to dry spells. We find that El Niño (La Niña) has contradictory effects on MCDDs in different winter months in the southern half of the country. These findings are of great importance for a country like Iran that lies in arid and semi-arid regions, as they can be useful for water resources management.

**Keywords:** MCDDs, dry spells, satellite data, linear trend, ENSO, Iran.

39 **Introduction**

40 The increase in anthropogenic greenhouse gas concentrations has led to drying conditions in the  
41 Northern Hemisphere subtropics and tropics (Zhang et al., 2007; Min et al., 2011). During recent  
42 decades, precipitation has tended to decrease in the Northern Hemisphere subtropical zones (IPCC,  
43 2007). The changes in precipitation regime had significant effects on arid and semi-arid regions,  
44 such as Iran.

45 One approach towards understanding precipitation characteristic is the study of dry spells, which  
46 gives a better characterization of the dry season than the sum of precipitation amount  
47 (Douguedroit, 1987). The dry spells are defined as a number of consecutive days without  
48 precipitation that affect extended areas (Anagnostopoulou et al., 2003; McCabe et al., 2010). In  
49 definitions of dry spells, there are various precipitation per day thresholds. Martin-Vide and  
50 Gomez (1999) used that of daily rainfall more than or equal to 10 mm threshold. Other studies  
51 used different threshold values such as 0.1, 1 and 10 mm (Kutiel, 1985; Kutiel and Maheras, 1992;  
52 Anagnostopoulou et al., 2003), and more than or equal to 5 mm (Serra et al., 2006; Lana et al.,  
53 2008). Dry spells may greatly affect soil moisture, snowpack, streamflow, groundwater, reservoir  
54 storage, and bring devastating damage to crops (Seleshi et al., 2006; Caloiero et al., 2015). The  
55 study of the occurrence of dry spells is therefore important in managing water resources and  
56 understanding the impact of climate change on droughts (Singh and Ranade, 2010; Deni et al.,  
57 2010; Llano and Penalba, 2011).

58 Several previous studies investigated the trend of dry spells in various parts of the world and  
59 obtained contradictory results in spatial and temporal scales. Seleshi and Camberlin (2006) found  
60 no trends in the yearly maximum length of dry spells over Ethiopia. Many studies have observed  
61 a decreasing trend in dry spell periods in the winter season, such as Suppiah and Hennessy (1998)  
62 in Australia, Serra et al. (2006) in Catalonia (Spain), Deni et al. (2010) over Peninsular Malaysia,  
63 McCabe et al. (2010) in the southwestern United States, Duan et al. (2017) in China,. On the  
64 contrary, some studies observed an increasing trend in winter dry days, for example, Schmidli and  
65 Frei (2005) in Switzerland, Sang et al. (2015) in Peninsular Malaysia, and Caloiero et al. (2015)  
66 in southern Italy.

67 Numerous studies have reported a significant relationship between dry spells and teleconnection  
68 patterns in different parts of the world (Bonsal and Lawford, 1999 in the Canadian Prairies;  
69 Barrucand et al., 2007 in Argentina; Oikonomou et al., 2010 in Eastern Mediterranean; Unalet al.,  
70 2012 in Turkey; Wang et al., 2015 in the arid region of China; Raymond et al., 2018 over the  
71 Mediterranean basin).

72 Several studies have been performed regarding precipitation trends in Iran. Modarres and Sarhadi  
73 (2009) found that negative trends of annual rainfall are mostly observed in northern and  
74 northwestern regions. Tabari and Talaei (2011) showed that significant negative trends occurred  
75 mostly in the northwest of Iran. Abarghouei et al. (2011) indicated a significant negative trend of  
76 drought in many parts of Iran, especially the southeast, west and southwest regions of the

77 country. Some'e et al. (2012) showd decrease in the winter precipitation series in northern Iran, as  
78 well as along the coasts of the Caspian Sea. Raziei et al. (2014) found that the precipitation is  
79 decreasing in spring and summer and increasing in autumn and winter in most of Iran. Najafi and  
80 Moazami (2016) showd an overall declining trend of the annual precipitation, in particular in  
81 regions located on the north, west and northwest of Iran. The seasonal analysis shows the largest  
82 contribution of winter to this declining trend. Asakereh (2017) indicated that there were major  
83 declining changes in precipitation in the northwest of Iran. Numerous studies showed a significant  
84 relationship between precipitation in Iran and various teleconnection patterns such as SOI  
85 (Nazemosadat and Cordery, 2000.a; Nazemosadat and Cordery, 2000b; Araghi et al., 2016;  
86 Dehghani et al., 2020), ENSO (Mariotti, 2007; Hosseinzadeh et al., 2014; Biabanaki et al., 2014);  
87 Alizadeh-Choobari et al., 2018), the NAO (Dezfuli et al., 2010; Araghi et al., 2016), AO (Araghi  
88 et al., 2016), the PDO (Biabanaki et al., 2014) and the SCN pattern (Ahmadi et al., 2019).

89 The results of a study of MCDDs are different compared to rainfall. Sivakumar MVK (1992) and  
90 Cindrić et al. (2010) pointed out that relying only on the precipitation amount can sometimes lead  
91 to incorrect conclusions because if heavy precipitation is recorded after a long dry spell, one might  
92 assume that the analyzed period was wet, while this was not the case. For Iran, Nasri and Modarres  
93 (2009) revealed individual trends of dry spells in the Isfahan Province, however so far  
94 no comprehensive study has been conducted in this regard.

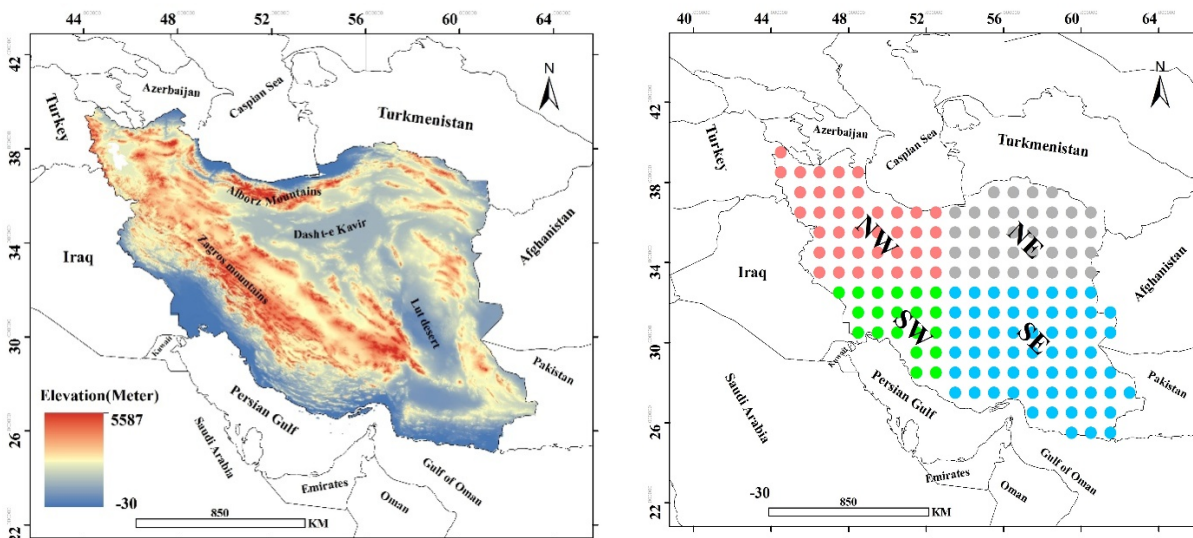
95 One of the benefits of this research is the use of precipitation from satellite data. The advantage of  
96 satellite data is that they have full spatial coverage and can also provide data for Iranian deserts  
97 (which do not have meteorological stations). Recent findings by Brocca et al. (2020) indicated  
98 that, particularly over scarcely gauged areas, integrated satellite products outperform both ground-  
99 and reanalysis-based rainfall estimates. Additionally, Darand et al. (2017) showed that the TRMM  
100 precipitation data in Iran has high potential in regions where rain gauge observations are  
101 nonexistent. Therefore, this study is the first comprehensive study on MCDDs over Iran. The  
102 results of this research are presented in three separate sections. First, we focus on the spatial  
103 characteristics of the MCDDs over Iran. Then, the results obtained from the MCDDs trend analysis  
104 are presented and finally, the relationship between the MCDDs and the ENSO teleconnection  
105 pattern is examined.

106

## 107 **Study area**

108 Iran is located in the subtropical arid belt of the northern hemisphere and covers an extensive area  
109 of 1648000 km<sup>2</sup> (Fig. 1, left panel) (Hosseinzadeh, 2004; Modarres, 2006). The annual  
110 rainfall in Iran is 250 mm, that is less than the global average (Raziei et al., 2014). The two major  
111 mountain ranges in Iran are Alborz in the north and Zagros in the west, while the main deserts of  
112 Iran are Dasht-i-Kavir and Dasht-e Lut (Shenbrot et al., 1999). In this study, the satellite  
113 precipitation data obtained are based on 156 1° latitude × 1° longitude grid points within the Iran  
114 borders (Fig. 1, right side). In order to better interpret the results in different geographical regions  
115 of Iran, we divided the country into 4 parts based on gridded points, including Northwest (NW),

116 Northeast (NE), Southwest (SW) and Southeast (SE). This division was made due to the diversity  
117 of Iran's climate in these areas and it is helpful for a better presentation of the results.



118 **Fig 1.**The geographical location of the study area. Topographic conditions (left panel) and classification of 1°  
119 latitude × 1° longitude points into different geographical areas (right panel).  
120

## 121 Data and methods

122 In this study, we obtained 22 years (1998 to 2019) of daily precipitation data from TRMM  
123 (3B42\_Daily v7) for winter months (Dec, Jan, Feb and Mar) from the Giovanni interface  
124 (<http://giovanni.gsfc.nasa.gov/giovanni/>). The reason for choosing the winter months was due to  
125 the fact that more than half of the annual precipitation in Iran occurs during this season (Domroes  
126 et al., 1998). The TRMM rainfall data were resampled to a 1° spatial resolution and considering  
127 the one-degree distance, 156 points were examined (Fig. 1, right side). Then, the MCDDs were  
128 calculated for each of the winter months from December to March. In this study, the MCDDs are  
129 defined as the longest period of consecutive days, during which no precipitation occurred. After  
130 extracting the MCDDs for all points, their temporal and spatial characteristics were examined  
131 separately for each month. In the next step, the magnitude of trends was derived using linear  
132 regression. Finally, the Spearman correlation was used in order to measure the relationship  
133 between the MCDDs and the ENSO teleconnection pattern. The teleconnection pattern index used  
134 in this study is the multivariate ENSO index, which was obtained from the Climate Prediction  
135 Center website (<http://www.cpc.ncep.noaa.gov/data/teledoc/telecontents.shtml>).

137 As we wanted to observe whether there is spatial homogeneity in the correlation coefficients  
138 between the ENSO and MCDDs, the spatial autocorrelation index was used. Spatial  
139 autocorrelation is the correlation among values of a single variable with itself in geographic space  
140 (Griffith 2003). The spatial autocorrelation can be calculated by various spatial statistics such as  
141 Moran's I (Moran, 1950) that was used here:

142

$$(1) I = \frac{\sum_{i=1}^n (x_i - \bar{x}) \sum_{j=1}^n w_{ij} (x_j - \bar{x}) / \sum_{i=1}^n \sum_{j=1}^n w_{ij}}{\sum_{i=1}^n (x_i - \bar{x})^2 / n}$$

143 Where  $x_i$  is the observed correlation coefficient at point  $i$ ,  $\bar{x}$  is the average of all correlation  
 144 coefficients over the  $n$  points, and  $w_{ij}$  is the spatial weight between two points  $i$  and  $j$ .  
 145 Here  $w_{ij}$  takes a nonzero value if the two locations are neighbors and zero otherwise. In the right-  
 146 hand part of Eq. (1), all weights are stored in the spatial weight matrix. In this study, the spatial  
 147 autocorrelation will be referred to as Moran's I. Moran's I values vary between  $-1$  and  
 148  $1$ . Values of Moran's I larger than expected (perfect positive correlation) mean that values tend to  
 149 be similar and values smaller than expected (perfect positive correlation) reveal that they tend to  
 150 be dissimilar (Griffith 2003).

151 After calculating the correlation coefficient, the points with the most significant values were  
 152 identified. Then, the relationships between MCDDs and atmospheric variables, such as Sea Level  
 153 Pressure (SLP), geopotential height, wind and specific humidity were investigated. For this,  
 154 reanalysis data from the NCEP/NCAR (National Centers for Environmental Prediction/National  
 155 Center for Atmospheric Research) were used (Kalnay et al., 1996). To investigate the effect of  
 156 ENSO on the MCDDs anomalies, the strongest El Niño and La Niña years were identified  
 157 separately for each month (Table 1), and mean anomaly maps were compared for each phase. The  
 158 5 strongest El Niño (La Niña) years were obtained after sorting the ENSO index to compare the  
 159 MCDDs lengths during the most pronounced warm and cold phases. Anomalies of MCDDs and  
 160 reanalyses data for each month were calculated using Z-scores. Then the monthly average of  
 161 standard scores for the years of El Niño and La Niña was calculated (see Table 1 for the years used  
 162 in each case). The aim is to find out whether there is a significant difference between the values of  
 163 MCDDs, as well as of the different atmospheric variables, when comparing the El Niño and La  
 164 Niña phases. For this purpose, a one-way analysis of variance was used. A paired t-test was  
 165 performed to compare the differences in MCDDs lengths between all 22 years and the 5 El Niño  
 166 (La Niña) years and calculate the statistical significance.

167 **Table 1- The strongest phases of Enso (El Niño and La Niña) in different years separately for each month.**

Month	Dec	Jan	Feb	Mar
El Niño	2002-2004-2006- 2009-2015	1998-2003-2007- 2010-2016	1998-2003-2005- 2010-2016	1998-2005-2010- 2016-2019
La Niña	1998-1999-2007- 2010-2011	1999-2000-2008- 2011-2012	1999-2000-2001- 2008-2011	1999-2000-2008- 2009-2011

168

169 **Results and discussion**

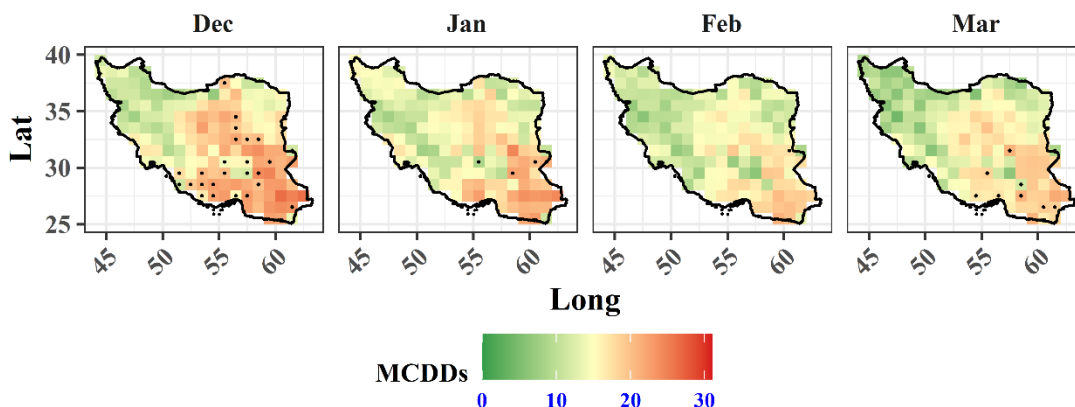
170 **The distribution of average monthly MCDDs**

171 Fig. 2 shows the mean monthly MCDD length for each grid point in Iran (grid points with high  
172 standard deviation are marked) Dec to Mar for the study period 1998-2019. As mentioned, in  
173 order to better analyze the spatial distribution of MCDDs, Iran is divided into four separate  
174 regions: the northeast, northwest, southeast and southwest. In general, the monthly maximum and  
175 minimum average MCDDs is observed during Dec ( $15.8 \pm 6.4$ ) and Feb ( $12.8 \pm 5.2$ ), respectively.  
176 Table 2 presents some of the statistical characteristics of the MCDDs values from Dec to Feb for  
177 the 4 geographical regions of Iran.

178 In Dec, the maximum and minimum spatial values of MCDDs are observed in the southeastern  
179 ( $20.4 \pm 7.6$ ) and in the northwest region ( $11.7 \pm 4.7$ ), respectively. During Dec  
180 the maximum amount of MCDDs is observed on the southeastern region (MCDDs= 26.5)  
181 (at latitude  $27.5^\circ$  and longitude  $60.5^\circ$ ), while the minimum value is located in northeastern Iran  
182 (MCDDs= 6.9) (at latitude  $36.5^\circ$  and longitude  $54.5^\circ$ ). In January, the maximum and minimum  
183 spatial values of MCDDs are observed in the southeast ( $17.9 \pm 6.7$ ) and in the northwest ( $12.6$   
184  $\pm 5.5$ ), respectively. In this month, the amount of MCDDs in the southwestern region of Iran is 12.8  
185 (5.5). Therefore, in January, there is no significant difference between the northwestern and  
186 southwestern regions of Iran. In general, MCDDs in the western half are fewer, compared to the  
187 eastern half. In January the maximum amount of MCDDs was observed on the southeastern region  
188 (MCDDs= 24.6) (at latitude  $31.5^\circ$  and longitude  $58.5^\circ$ ), while the minimum value is located in  
189 southwestern Iran (MCDDs= 7.8) (at latitude  $31.5^\circ$  and longitude  $50.5^\circ$ ). In Feb, the maximum  
190 and minimum spatial values of MCDDs are observed in the southeast ( $15.9 \pm 6.4$ ) and in the  
191 northwest ( $10.9 \pm 4.6$ ), respectively. During Feb the maximum amount of MCDDs was observed  
192 in the southeastern region (MCDDs= 21.1) (at latitude  $25.5^\circ$  and longitude  $59.5^\circ$ ), while the  
193 minimum value is located in northwestern Iran (MCDDs= 6) (at latitude  $34.5^\circ$  and longitude  $47.5$   
194  $^\circ$ ). Finally, in March, similarly to previous months, the maximum and minimum spatial values of  
195 MCDDs are observed in the southeast ( $17 \pm 6.7$ ) and in the northwest ( $9.6 \pm 4.2$ ), respectively.  
196 During March the maximum amount of MCDDs was observed on the southeastern region  
197 (MCDDs= 21.8) (at latitude  $27.5^\circ$  and longitude  $61.5^\circ$ ), while the minimum value is located in  
198 northwestern Iran (MCDDs= 4.2) (at latitude  $34.5^\circ$  and longitude  $47.5^\circ$ ).

199 Based on the above results, the highest (lowest) values of MCDDs occur in the southeast  
200 (northwest) in all months. This is in contrary to the findings of drought-related research but similar  
201 to the results obtained from the distribution of rainfall values in Iran. Bazrafshan and Khalili  
202 (2013) showed that drought phenomena can occur both in the northwest and in the southeast of the  
203 country. According to the study of Ashraf et al. (2014) Rasht (at the southern Caspian Sea) had  
204 the highest and Yazd (at the Southeast region in this study) had the lowest amount of total  
205 precipitation over Iran. In general, the frequency of rainy days in southeastern Iran is low and vice  
206 versa in the northwest, especially at the southern shores of the Caspian Sea, where the frequency  
207 of occurrence is very large. Nazaripour and Daneshvar (2014) reported that one-day  
208 precipitation generates the maximum annual precipitation amounts in eastern parts of Iran. Razinei

209 et al. (2014) showed that the maximum number of rainy days are observed in the Caspian Sea  
 210 region.



211  
 212 **Fig. 2- Spatial distribution of monthly average length of MCDDs during 1998-2019 over Iran (the marked**  
 213 **grid points show points with relatively high standard deviation (above 8.))**  
 214

215 **Table 2- Characteristics of descriptive statistics of MCDDs in the geographical areas of Iran separately for**  
 216 **each month.**

Month	Region	Mean	SD	Max	Min
Dec	SW	14.4	6.5	19.1	9.2
	SE	20.4	7.6	26.5	11.5
	NW	11.7	4.7	18.0	7.7
	NE	16.6	6.7	22.6	6.9
	All	15.8	6.4	26.5	6.9
Jan	SW	12.8	5.5	17.1	7.8
	SE	17.9	6.7	24.6	8.5
	NW	12.6	5.5	16.0	7.9
	NE	14.5	5.6	18.7	8.9
	All	14.5	5.8	24.6	7.8
Feb	SW	11.3	4.8	15.4	6.9
	SE	15.9	6.4	21.1	6.2
	NW	10.9	4.6	14.7	6.0
	NE	13.1	5.3	17.0	8.5
	All	12.8	5.2	21.1	6.0
Mar	SW	12.2	5.2	16.1	5.9
	SE	17.0	6.7	21.8	6.3
	NW	9.6	4.2	16.1	4.2
	NE	13.8	5.5	19.8	5.5
	All	13.2	5.4	21.8	4.2

217

218 **Analysis of MCDDs trend**

219 In Fig. 4, the positive and negative coefficients of the linear trend are mapped for the months of  
 220 Dec to Mar. In general, the average coefficients from Dec to Mar are 0.18, 0.25, 0.17, and 0.08,  
 221 respectively. In all months, the frequency of points with positive coefficients is significantly higher  
 222 than that of points with negative coefficients. The number of points with positive (negative)

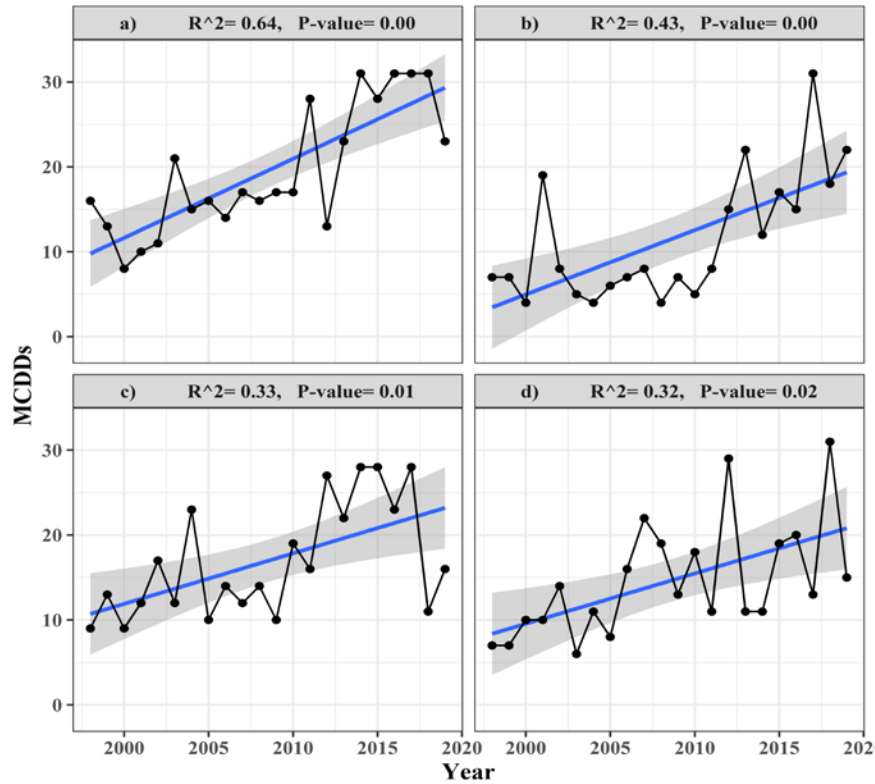


223 coefficients for January to March is 121 (33), 133 (22), 137 (16), and 105 (49), respectively. Fig.  
224 4 shows the points with a significant trend along with their coefficients of determination. The  
225 number of points with a significant trend of the MCDDs in Iran for Dec to Mar is 33, 38, 22 and  
226 13, respectively. In all months, the highest number of points with a significant trend in the MCDDs  
227 are observed in northwestern and southeastern Iran. For example, during Dec, 18 points (with a  
228 one-degree spatial resolution) had a significant increasing trend in the northwest, while in the same  
229 month, 14 points had a decreasing trend in the southeast region.

230 These results are exactly in line with the findings of Golian et al. (2015). They showed that the  
231 northern, northwestern, and central parts of Iran have significant drying trends, while, there is no  
232 statistically significant drying trend in the eastern part of the country. In general, statistical  
233 significant trends in the MCDDs are more concentrated in the northern half of the country  
234 (especially in NW) than in the southern half. This is similar to previous results obtained for  
235 precipitation trends over Iran. Modarres and Sarhadi (2009); Tabari and Talaei (2011); Some'e, et  
236 al. (2012); Najafi and Moazami (2016) and Asakereh (2017) all found decreasing trends of  
237 precipitation in northern and northwestern regions.

238 In December, an increasing trend in the number of MCDDs can be seen in all regions of the  
239 country. The highest and lowest values of the average coefficients were observed in the northwest  
240 (0.25) and southeast (0.04), respectively. In this month, the highest value of the coefficient is 0.64  
241 in the center of Iran (at latitude  $32.5^{\circ}$  and longitude  $54.5^{\circ}$ , Fig.3.a) and its lowest value is -0.53 in  
242 southeastern Iran (at latitude  $31.5^{\circ}$  and longitude  $60.5^{\circ}$ ). In January, the spatial pattern of the  
243 coefficients is similar to December. MCDDs have an increasing trend in most parts of the country.  
244 In general, the average trend coefficient in southwestern Iran is higher than in other regions (0.32).  
245 Significant declining trends are also confirmed in the southeast, and significant increases are  
246 observed in parts of the central, southeastern, and western regions. Fig.3, b shows the increasing  
247 trend with coefficient 0.43, at latitude  $28.5^{\circ}$  and longitude  $51.5^{\circ}$ . In February, the number of points,  
248 which have a decreasing trend, reach the minimum number. However, in some points of the  
249 southeast, there is a decreasing trend in the MCDDs. In other parts of the country an increasing  
250 trend in the MCDDs can be seen during Feb. Fig.3, c shows the point with the maximum  
251 increasing trend ( $R^2= 0.33$ ) in the central region of Iran (at latitude  $34.5^{\circ}$  and longitude  $54.5^{\circ}$ ).  
252 Finally, in Mar, similar to the previous months, there is a decreasing trend in the southeastern  
253 region and an increasing trend in other parts of the country. Significant trends are concentrated in  
254 the central parts of the country as well as in some parts of the southeast and west of Iran. During  
255 Mar, the highest value of the coefficient is 0.32 in the center of Iran (at latitude  $33.5^{\circ}$  and longitude  
256  $51.5^{\circ}$ , Fig.3.d).

257



258  
259  
260  
261

Fig. 3- MCDDs trends for the gridpoints with the maximum coefficients of determination. a) At latitude 32.5° and longitude 54.5 °. b) At latitude 28.5° and longitude 51.5°. c) At latitude 34.5° and longitude 54.5. d) At latitude 33.5° and longitude 51.5 °.

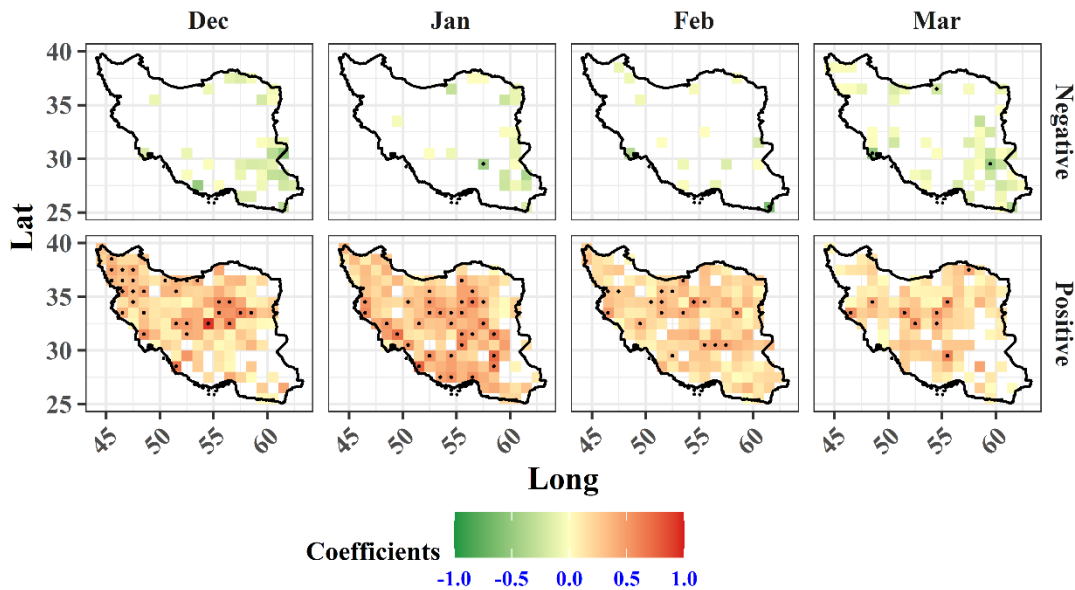


Fig. 4- Spatial distribution of monthly negative (top row) and positive (bottom row) MCDDs linear trend during 1998-2019 over Iran (the marked grid points show a statistically significant coefficient for  $p < 0.05$ ).

262

## 263 **The relationship between MCDDs and ENSO**

264 In Fig. 5, the values of the correlation coefficients between MCDDs and the ENSO teleconnection  
265 pattern are mapped. As can be seen in the map, the significant correlation coefficients are negative  
266 in December and March, but positive in January and February.

267 In Table 3, the Moran's I values for the spatial correlation coefficients between the MCDDs and  
268 ENSO are presented separately for each month. The Moran's I can show how the values of the  
269 correlation coefficients are distributed spatially (in Fig 5). Low values of Moran's I show that the  
270 positive and negative correlation coefficients are irregularly distributed over the country, which  
271 means that it cannot be said that the ENSO has the same effect on the MCDDs variation during  
272 various months. Next, the relationships between MCDDs and ENSO values have been investigated  
273 in the winter months.

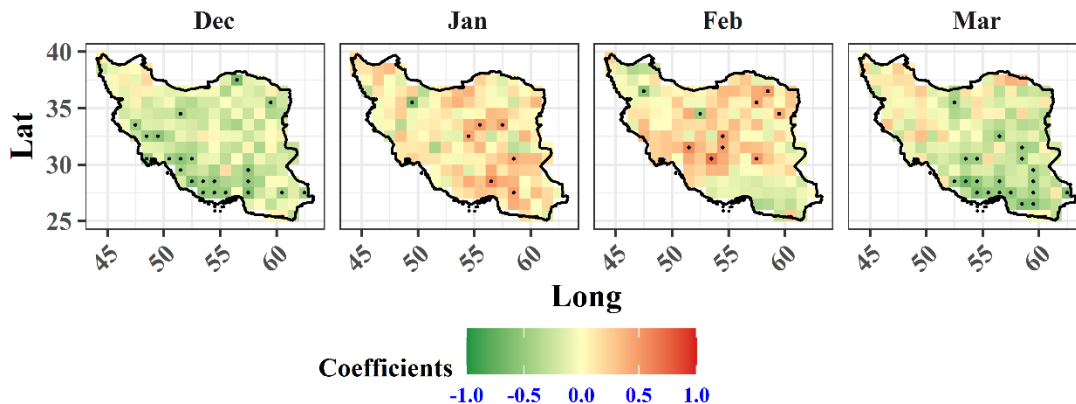
274 **Table 3. Moran's I values for correlation coefficients between MCDDs and the ENSO teleconnection pattern**

Month	Dec	Jan	Feb	Mar
<b>Moran I</b>	0.16	0.19	0.39	0.35

275  
276 In December, the ENSO showed an inverse relationship with MCDDs in southwestern Iran, but  
277 regarding the value of Moran index (0.16), its effects have a low spatial homogeneity compared to  
278 other months. In December, all significant correlation coefficients are negative and are often  
279 located in the southwestern region. In January, the Moran value is 0.19. The average correlation  
280 coefficients in the southeast (0.15) are higher than in other regions and the maximum is 0.57. The  
281 Moran's index in February shows that the spatial homogeneity of the correlation coefficients is  
282 higher compared to the other months. In the northeast and southwest, the coefficients are mostly  
283 positive. For example, in the southwest, the average correlation coefficient is 0.25. However, in  
284 the southeast and northwest, several points have a negative coefficient. As mentioned, in February,  
285 the relationship between MCDDs and the ENSO index is often positive in different parts of Iran.  
286 The positive and significant correlation coefficients are observed from southwest to northeast.

287 The length of the MCDDs has also increased as the value of the ENSO index increases. In  
288 February, there is also a negative correlation in some parts of the southeast and northwest. The  
289 strongest coefficient can be seen at latitude  $37.5^\circ$  and longitude  $45.5^\circ$ , ( $r = -0.57$ ). According to  
290 the correlation coefficient values, during February the lowest and highest amount of relationship  
291 between the ENSO index and MCDDs were obtained in southwest at latitude  $30.5^\circ$  and longitude  
292  $53.5^\circ$  ( $r = 0.66$ ), and in northwest at latitude  $36.5^\circ$  and longitude  $47.5^\circ$  ( $r = -0.57$ ), respectively. In  
293 March, the Moran coefficient is 0.35 and the ENSO has an effect on the amount of MCDDs. In  
294 general, in most parts of Iran, there is a negative relationship ( $r = -0.15$ ) and its highest is  $-0.69$ .  
295 Also, in the northwest, the average coefficients are negative ( $r = -0.02$ ), but this relationship is  
296 weaker than in other regions. The positive ENSO values are related to El Niño events (warm phase)  
297 which is connected to wetter conditions over most regions of Iran according to various studies  
298 (Nazemosadat et al., 2000,a; Hosseinzadeh Talaei et al., 2014; Biabanaki et al., 2014; Alizadeh-  
299 Choobari et al., 2018; Ahmadi et al., 2019). Indeed, it is found that in the warm phases of ENSO,

300 the length of the MCDDs has decreased, which is consistent with previous studies. The negative  
 301 coefficients are more abundant in December than in other months. Mariotti (2007) reveals that the  
 302 ENSO impact on precipitation of southwest Asia is highest during the transition seasons of autumn  
 303 and spring. In March, the lowest and highest amount of the relationship between the ENSO index  
 304 and MCDDs was obtained in the south (at latitude  $28.5^\circ$  and longitude  $53.5^\circ$ ,  $r = -0.69$ ), and in  
 305 the northeast (at latitude  $37.5^\circ$  and longitude  $57.5^\circ$ ,  $r = 0.37$ ), respectively. Table 4 shows the  
 306 average and maximum correlation coefficients between MCDDs and ENSO for the four different  
 307 regions.



308  
 309 **Fig. 5- The correlation coefficients between MCDDs values and ENSO separately for December to March**  
 310 **(The marked grid points show a statistically significant coefficient for  $p < 0.05$ ).**  
 311

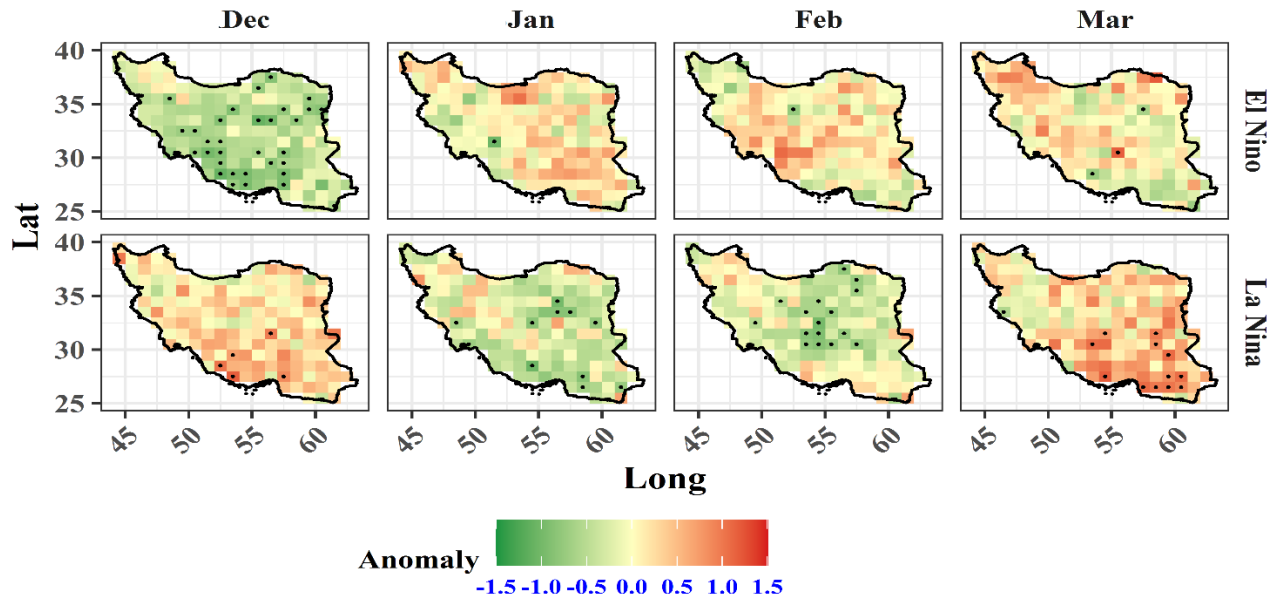
312 **Table 4- Mean and maximum values of the correlation coefficients between MCDDs and ENSO in the 4**  
 313 **geographical areas of Iran and over the whole country.**

Month	Region	ENSO vs. MCDDs	
		Mean	Max
Dec	SW	-0.33	-0.59
	SE	-0.21	-0.61
	NW	-0.12	-0.46
	NE	-0.19	-0.65
	All	-0.20	-0.65
Jan	SW	0.05	-0.41
	SE	0.15	0.57
	NW	0.03	-0.60
	NE	0.14	0.50
	All	0.11	-0.60
Feb	SW	0.25	0.58
	SE	0.02	0.66
	NW	-0.01	-0.57
	NE	0.17	0.49
	All	0.08	0.66
Mar	SW	-0.10	-0.46
	SE	-0.29	-0.69
	NW	-0.02	-0.45
	NE	-0.08	0.39
	All	-0.15	-0.69

314  
 315 **Comparison of MCDDs anomalies in El Niño and La Niña periods**  
 316 In the previous section, it was observed that the effect of the Multivariate ENSO Index (MEI) on  
 317 the MCDDs variability can differ from one winter month to another. We calculated the correlation

318 coefficients between the MCDDs and other ENSO indicators such as Niño 1+2, Niño 3.4, Niño 4  
319 and SOI. In all cases, this contradiction was observed (not shown). In this section, the MCDDs  
320 anomalies in the five years with negative phase (La Niña) and the five years with positive phase  
321 (El Niño) are compared separately for each month (Fig. 6). The results of analysis of variance  
322 showed that there is a significant difference between the anomaly of MCDDs when comparing  
323 each month separately in the El Niño and La Niña phases (Table 5 and 6). In December, the  
324 average anomaly (in Iran) in the El Niño and La Niña phases is  $-0.45 (\pm 0.29)$  and  $0.25 (\pm 0.33)$ ,  
325 respectively. This indicates that in the warm phases of ENSO the length of the MCDDs was shorter  
326 than in the cold phases. In January, the average anomalies in the El Niño and La Niña phases were  
327  $0.11 (\pm 0.35)$  and  $-0.24 (\pm 0.37)$ , respectively. Therefore, in the warm phases of El Niño, not only  
328 has the length of dry periods not decreased, but it has also had a positive anomaly. In February,  
329 the situation is the same as in January. In the El Niño phases, the anomaly value is very small,  $0.09$   
330  $(\pm 0.35)$ , but in the La Niña phases, the anomaly value is  $-0.2 (\pm 0.34)$ . In March, the anomalies  
331 were positive in both El Niño and La Niña phases. However, the amount of anomaly in El Niño  
332 ( $0.08, \pm 0.38$ ) is insignificant compared to La Niña ( $0.33, \pm 0.41$ ). In Fig. 6, the black circles on the  
333 MCDDs anomaly values show the points with statistical significant differences (at the 5% level)  
334 between the long-term (22 years) MCDDs values compared to their values during El Niño and  
335 La Niña phases based on the t-test. In the El Niño years, the most significant differences are  
336 observed for December (at 32 points) from southwest to northeast, but in the other months the  
337 number of significant points is very small. However, significant differences can be seen in all  
338 months in the La Niña years. The significant differences are negative in January and February but  
339 positive in December and March. Therefore, the contradiction in the MCDDs length (between  
340 January-February with December-March) is stronger during the La Niña compared to the El Niño  
341 periods.

342 These results are consistent with the results obtained from the correlation coefficients and they  
343 confirm the contradiction of the relationship between MCDDs and ENSO in January-February  
344 compared with December-March. Therefore, in terms of the MCDDs anomalies, in general,  
345 January and February have a positive relationship, and December and March have a negative  
346 relationship with the ENSO index. The largest differences in correlation values between the El  
347 Niño and La Niña phases are observed for December ( $0.71$ ) and January ( $-0.35$ ), respectively. In  
348 addition, in the El Niño phases, there is a difference between the anomaly values in different  
349 months, with the most significant difference between January and December ( $0.56$ ). However, the  
350 difference between January and February in the years of El Niño is negligible ( $-0.01$ ) (Table 5).



351  
 352 **Fig. 6- Comparison of MCDDs anomalies in five years of positive and five years of negative phases of the**  
 353 **ENSO index. Top row El Niño , bottom row La Niña. Marked grid points show statistically significant**  
 354 **differences for  $p < 0.05$  based on t-test when comparing El Niño (La Niña) with all years.**  
 355

356  
 357  
 358 Table 5 shows the average of MCDDs anomalies during El Niño and La Niña years separately in  
 359 different geographical areas of Iran. As can be seen in the table, during El Niño years, negative  
 360 anomalies are observed only in December in all areas. But the amounts of MCDDs anomalies in  
 361 January, February, and March are often positive. The greatest difference can be seen between  
 362 December (-0.67) and February (0.47) in southwestern Iran. In the La Niña years in December and  
 363 March, there are positive anomalies in all regions, but stronger in the southern half (positive  
 364 anomalies are very weak in the northwest), while in January and February, the negative anomalies  
 365 are predominant in the country (except in the northwest). The greatest differences in anomalies  
 366 can be seen between January (-0.31) and March (0.55) in the southeast.

367 In La Niña phases, there is also a significant difference between anomalies in different months.  
 368 The highest and lowest differences can be seen for March and January (0.57) and February-January  
 369 (0.03), respectively (Table 6). In the following steps, for better analysis, the anomalies of the  
 370 atmospheric data were analyzed for January and December only and separately for the El Niño  
 371 and La Niña phases.

372

373  
 374  
 375  
 376  
 377  
 378

379 **Table 5- Average of MCDDs anomalies during El Niño and La Niña years separately in the four geographical**  
 380 **areas of Iran.**

Region	El Niño				La Niña			
	Dec	Jan	Feb	Mar	Dec	Jan	Feb	Mar
SW	-0.67	-0.16	0.47	0.22	0.31	-0.29	-0.24	0.22
SE	-0.45	0.22	0.05	-0.05	0.35	-0.31	-0.18	0.55
NW	-0.3	0.05	-0.03	0.22	0.15	-0.00	-0.04	0.09
NE	-0.5	0.14	0.1	0.09	0.16	-0.34	-0.38	0.28

381  
 382 **Anomalies of large-scale atmospheric variables in El Niño and La Niña periods**

383 According to the results obtained in the previous sections, the correlation coefficients as well as  
 384 the anomalies of MCDDs in the El Niño and La Niña periods in December and January showed  
 385 opposite results. In this section, to further analyze the cause of this contradiction, the anomalies of  
 386 large-scale atmospheric variables in the El Niño (Table 6) and LaNiña (Table 7) periods for  
 387 December and January are compared over Iran. In addition, the anomalous values are presented as  
 388 a pairwise comparison between different winter months. However, for brevity, comparisons have  
 389 been only made between January and December.

390 **Table 6- Anomaly comparison of MCDDs and large-scale variables in El Niño between winter months.**

variable	Month	Mean	SD	diff					
				Jan- Dec	Feb - Dec	Mar- Dec	Feb- Jan	Mar- Jan	Mar- Feb
MCDDs	Dec	-0.45	0.29	0.56**	0.55**	0.54**	-0.01	-0.02	-0.01
	Jan	0.11	0.35						
	Feb	0.09	0.35						
	Mar	0.08	0.38						
SLP	Dec	0.09	0.18	0.14	-	-0.08	0.31**	-0.23*	0.08
	Jan	0.23	0.35						
	Feb	-0.07	0.05						
	Mar	0.00	0.26						
hgt-500	Dec	-0.92	0.13	1.4**	0.72**	0.96**	0.66**	-	0.47**
	Jan	0.51	0.09						
	Feb	-0.14	0.05						
	Mar	0.04	0.12						
Uwnd-500	Dec	0.09	0.53	-0.29*	-0.18	0.13	-0.11	0.43**	0.31**
	Jan	-0.2	0.46						
	Feb	-0.08	0.04						
	Mar	0.23	0.08						
vwnd-500	Dec	0.49	0.57	-0.13	-0.22	-	0.31**	0.08	-0.18
	Jan	0.36	0.21						
	Feb	0.27	0.06						
	Mar	0.18	0.24						
shum-500	Dec	0.03	0.38	-0.06	0.00	0.64**	-0.07	0.71**	0.64**
	Jan	-0.03	0.43						
	Feb	0.04	0.24						
	Mar	0.68	0.18						

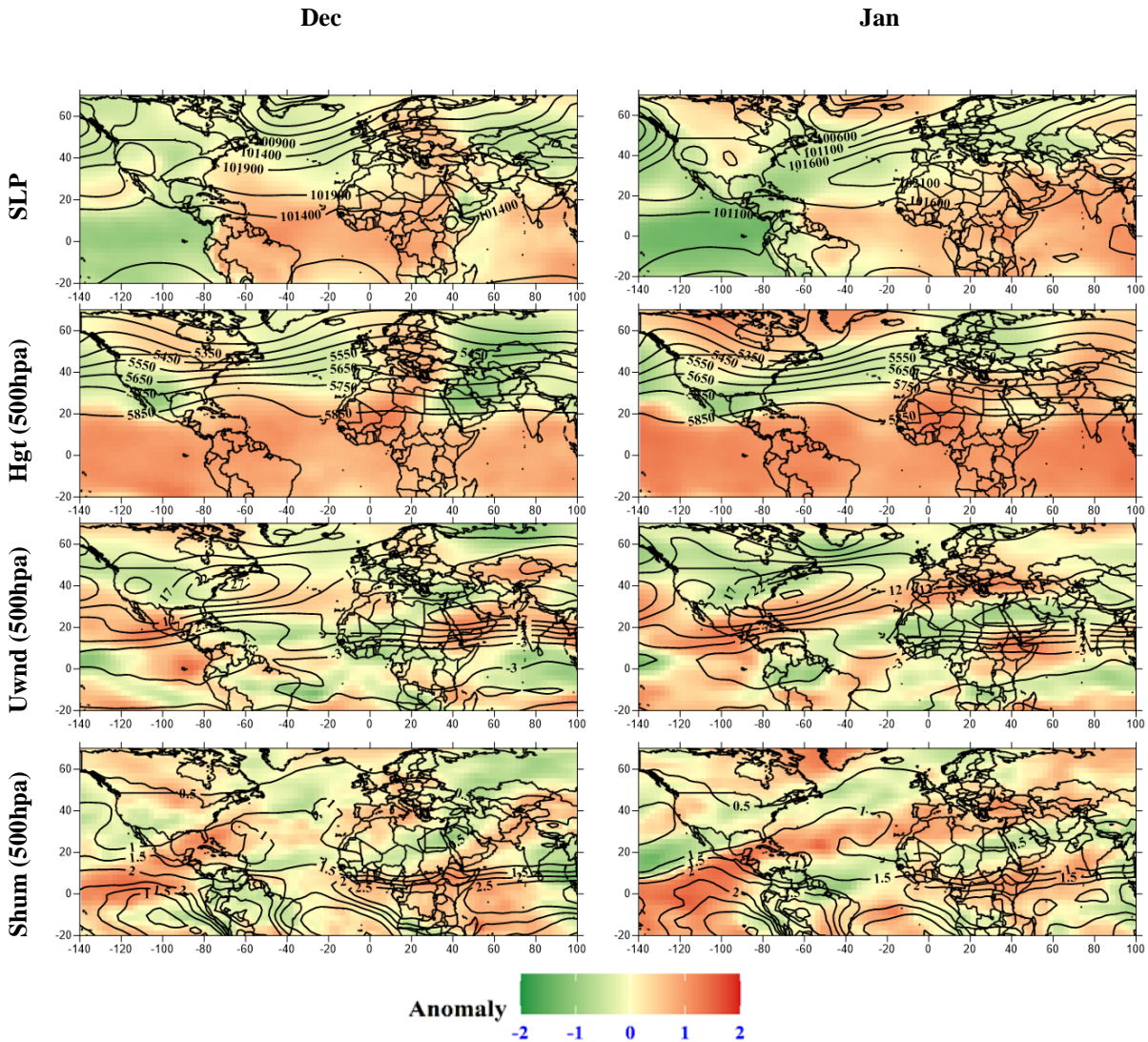
391 \*\* Significant at level of p=0.01 \* Significant at the level of p=0.05

392 **El Niño phases**

393 As seen in Table 6, during the El Niño phases, the geopotential height at the 500 hpa level, as well  
394 as the zonal wind component at the same pressure level, show significant differences in December  
395 and January (within the borders of Iran). The maximum difference in anomaly (1.4) is observed  
396 for the hgt-500. The 500-hpa negative anomalies in December and positive anomalies in January  
397 are seen in both the northern and southern half of the country (see Figure 7). As shown in Figure  
398 6 (top row), the positive (negative) anomalies in MCDDs length are observed during January  
399 (December) in both northern and southern halves. This suggests that during El Niño periods in  
400 December, hgt-500 appears at a lower height compared to the long term climatology. This leads  
401 to more cyclones as well as reduced MCDDs over Iran. On the contrary, in January, a positive  
402 anomaly of the geopotential height indicates that cyclones are less frequent and MCDDs are  
403 longer. Alijani (2002) and Raziei et al. (2012) concluded that the spatial distribution of  
404 precipitation over Iran depends on the geographical position of the mid-tropospheric trough over  
405 the Middle East, which links to the results shown. The zonal wind direction component also has  
406 completely different values for December and January. In December, a positive anomaly is seen  
407 (especially in the southern half of the country), but in January, a negative anomaly can be seen in  
408 almost all of Iran. A higher zonal wind component in December indicates that the wind direction  
409 was mostly westerly. This leads to the passage of cyclones, the occurrence of more precipitation,  
410 and finally the reduction of the length of MCDDs. However, in January, the zonal wind magnitude  
411 was below normal. The difference between zonal wind anomalies in December and January is  
412 greater (difference = -0.97) in the southern half of the country, compared to the northern half  
413 (difference = 0.65). During the El Niño years, the zonal wind anomalies in the southern and  
414 northern halves are reversed in both January and December. In December (January), the zonal  
415 wind anomalies are negative -0.38 (positive 0.27) in the northern half and positive 0.44 (negative  
416 -0.53) in the southern half. Ghasemi and Khalili (2008) found a significant positive correlation  
417 between zonal winds and winter precipitation over most parts of Iran. The meridional wind  
418 component has a significant difference in December and January (difference = -0.32) in the  
419 southern half of Iran. Although the anomaly is positive in both months, the anomaly values in  
420 December are larger than in January. However, the meridional wind component does not differ  
421 significantly between December and January in the northern half. The anomaly values of specific  
422 humidity at 500 hpa are 0.03 and -0.03 in December and January, respectively. Although the  
423 average humidity anomaly is not significantly different for the whole of Iran, the positive anomaly  
424 (0.21) in southern half in December and the negative anomaly (-0.2) in January are more  
425 pronounced. Similar to specific humidity, SLP does not show a significant difference for the whole  
426 country. However, there is a significant difference in the southern half in January when a relatively  
427 strong anomaly is seen in SLPs (0.47), while a weak negative anomaly is observed in the northern  
428 half at the same time. In general, in the El Niño years, when comparing December and January,  
429 the amount of MCDDs, as well as the anomalies of the hgt-500, in the northern and southern half  
430 do not differ significantly. However, zonal and meridian wind, SLP and humidity have different  
431 anomalies in the northern and southern half. In Fig. 7 anomalies of SLP, hgt-500, 500-hPa  
432 zonal wind and humidity are shown for January and December for the El Niño phases. The



433 negative anomaly at the hgt-500 and the positive anomaly in the zonal wind and humidity cause a  
 434 decrease in the length of MCDDs in December during the El Niño periods. On the contrary, the  
 435 hgt-500 is higher than normal in January, while zonal wind and humidity are lower than normal  
 436 and this synoptic situation leads to an increase in MCDDs during El Niño.



437 Fig 7. Comparison of anomaly values of large-scale atmospheric variables in El Niño phases between  
 438 December (left panel) and January (right panel).

439

440 Table 7- Anomaly comparison of MCDDs and large-scale variables in La Niña phases between winter  
 441 months.

variable	Month	Mean	SD	diff					
				Jan - Dec	Feb - Dec	Mar - Dec	Feb - Jan	Mar - Jan	Mar - Feb
MCD Ds	Dec	0.25	0.33						
	Jan	-0.24	0.37	-	-	0.07	0.03	0.57**	0.53**
	Feb	-0.2	0.34	0.49**	0.46**				

	Mar	0.33	0.41						
SLP	Dec	0.07	0.14	-	-0.04	-	-	-	-
	Jan	-0.21	0.39						
	Feb	0.02	0.08						
	Mar	-0.57	0.33						
				0.28**		0.64**	0.23**	0.35**	0.59**
hgt-500	Dec	0.67	0.11	-	-	-	-	-	-
	Jan	-0.72	0.08						
	Feb	-0.18	0.1						
	Mar	-0.13	0.04						
				1.39**	0.85**	-0.8**	0.54**	0.58**	0.04
Uwnd-500	Dec	-0.34	0.22	-	-	-	-	-	-
	Jan	0.24	0.58						
	Feb	0.43	0.13						
	Mar	-0.07	0.15						
				0.58**	0.78**	0.26**	-0.19	-0.32*	-
vwnd-500	Dec	-0.24	0.29	-	-	-	-	-	-
	Jan	0.15	0.29						
	Feb	-0.27	0.24						
	Mar	0.21	0.12						
				0.39**	-0.03	0.45**	0.43**	0.05	0.48**
shum-500	Dec	-0.66	0.23	-	-	-	-	-	-
	Jan	-0.06	0.69						
	Feb	-0.48	0.2						
	Mar	0.63	0.05						
				0.59**	0.18**	1.3**	0.41**	0.7**	1.1**

\*\* Significant at level of p=0.01

\* Significant at the level of p=0.05

442  
443  
444

## La Niña phases

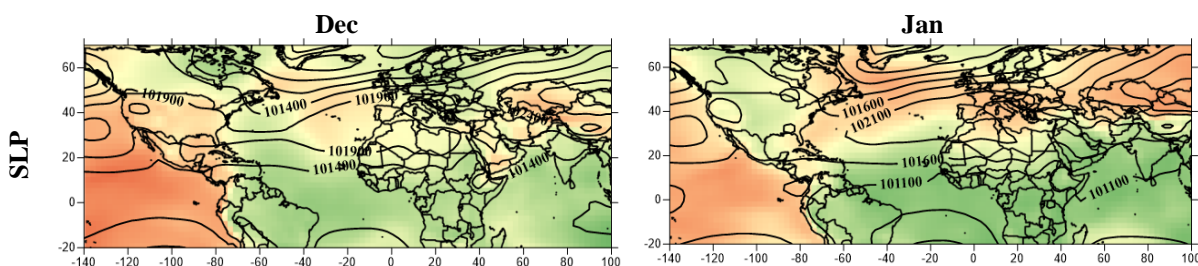
445 In the negative cold phases of ENSO (La Niña), the atmospheric parameters have significant  
446 differences in December and January (within the borders of Iran). Those differences between  
447 December and January are larger in the La Niña periods than in the El Niño periods in consistent  
448 with the MCDDs anomalies (see also black circles in Fig. 6). The highest anomaly difference  
449 between December and January (within the borders of Iran) is observed for the hgt-500 (-1.39),  
450 the values of 500-hpa specific humidity (0.59), 500-hpa zonal wind (0.58) and 500-hpa meridonal  
451 wind (0.39). The 500-hpa geopotential height for January and December during the La Niña years  
452 is exactly the opposite of the El Niño ones.

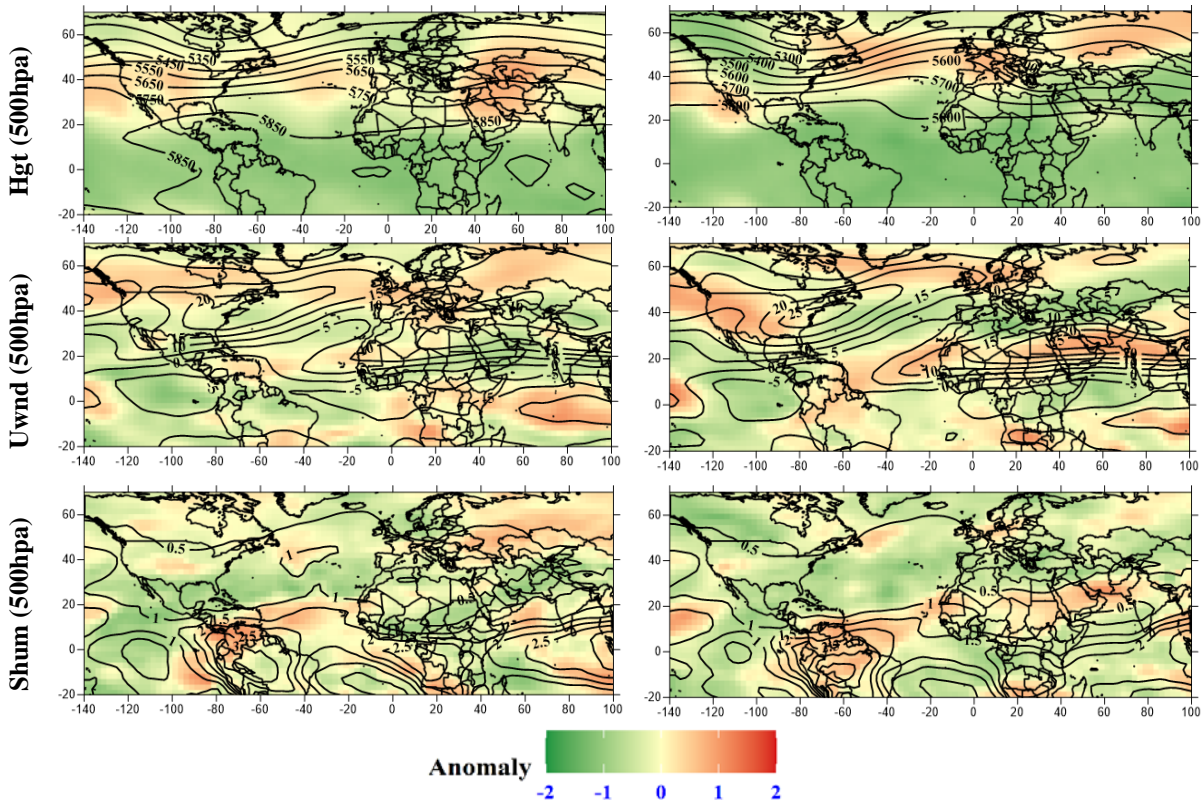
453 In the La Niña phases, the average anomaly at the hgt-500 for December and January is 0.67 and  
454 -0.72, respectively. This shows that in the La Niña periods during December, the hgt-500 is higher  
455 than the long-term situation, and vice versa, in January, it is lower than the long-term average in  
456 Iran (see also Fig. 8). The 500-hpa negative anomalies in December and positive anomalies in  
457 January are seen in both the northern and southern half of the country (see Figure 8). As shown in  
458 Figure 6 (bottom row), the negative (positive) anomalies in MCDDs length are observed during  
459 the January (December) in both the northern and southern halves. In the years of La Niña, the  
460 500-hpa zonal wind is completely different for December and January. In December, a negative  
461 anomaly ( $-0.34 \pm 0.22$ ) is seen in the zonal wind (except in a small part of the northwest). However,  
462 in contrast to the El Niño periods, a positive anomaly ( $0.24 \pm 0.58$ ) was observed in January,  
463 especially in the southern half of Iran. This positive anomaly of the 500-hPa zonal wind in January  
464 indicates that the wind flow was mostly westerly, which leads to more cyclones, more

465 precipitation, and a decrease in the length of the MCDDs. In December, however, the zonal wind  
 466 has a negative anomaly, and this has led to an increase in the length of the MCDDs. The difference  
 467 between zonal wind anomalies in December and January is significant only in the southern half  
 468 (difference = 1.15). Similar to the El Niño years, the zonal wind anomalies are reversed in both  
 469 January and December in the southern and northern halves during the La Niña years.

470 Unlike the El Niño years, during the La Niña periods, there is a significant difference in the values  
 471 of the 500-hPa meridional wind. In December, the 500-hPa meridional wind has a negative  
 472 anomaly ( $-0.24 \pm 0.29$ ), while in January it has a positive anomaly ( $0.15 \pm 0.29$ ). This shows that in  
 473 the La Niña periods during December, the meridional wind often had a northward direction, while  
 474 in January it often had a southward direction, which led to a decrease in the length of the MCDDs  
 475 in December and an increase in January. The meridional wind component has a significant  
 476 difference in December and January (difference = 0.46) in the southern half of Iran and the  
 477 anomaly is the opposite of that in the El Niño years. This indicates that in January, the wind often  
 478 tends to be southward during La Niña years in the southern half. Similar to the zonal wind,  
 479 Ghasemi, A. R., &Khalili, D. (2008) found significant positive correlation between meridional  
 480 winds and winter precipitation over most parts of Iran. The specific humidity anomaly is consistent  
 481 with the wind direction and the geopotential height. In December, the 500-hpa specific humidity  
 482 is negative in all regions of Iran ( $-0.66 \pm 0.23$ ). The negative specific humidity confirms the  
 483 increase in the length of MCDDs in the La Niña phases for December. In January the specific  
 484 humidity anomaly is positive in the southern half (0.35) and negative in the northern half (-0.76)  
 485 and this leads to an average anomaly close to zero over the whole country. Finally, SLP does not  
 486 show a significant difference in the northern half, but only in the southern half (difference= -0.54).  
 487 In January, a relatively strong negative anomaly is seen in SLPs (-0.45), while a weak positive  
 488 anomaly is observed in the northern half at the same time. Fig. 8 (similar to Fig. 7) compares the  
 489 anomaly values of sea level pressure, the hgt-500, zonal wind and specific humidity in the years  
 490 of La Niña for January and December. The positive anomalies at hgt-500 and negative anomalies  
 491 in the 500-hPa zonal wind and specific humidity lead to an increase in MCDDs during the La Niña  
 492 periods in December. However, in January, the hgt-500 has a negative anomaly, and at the same  
 493 time, the 500-hPa zonal wind and the specific humidity present a positive anomaly. These factors  
 494 combined lead to a decrease in the duration of MCDDs in January in the La Niña periods.

495



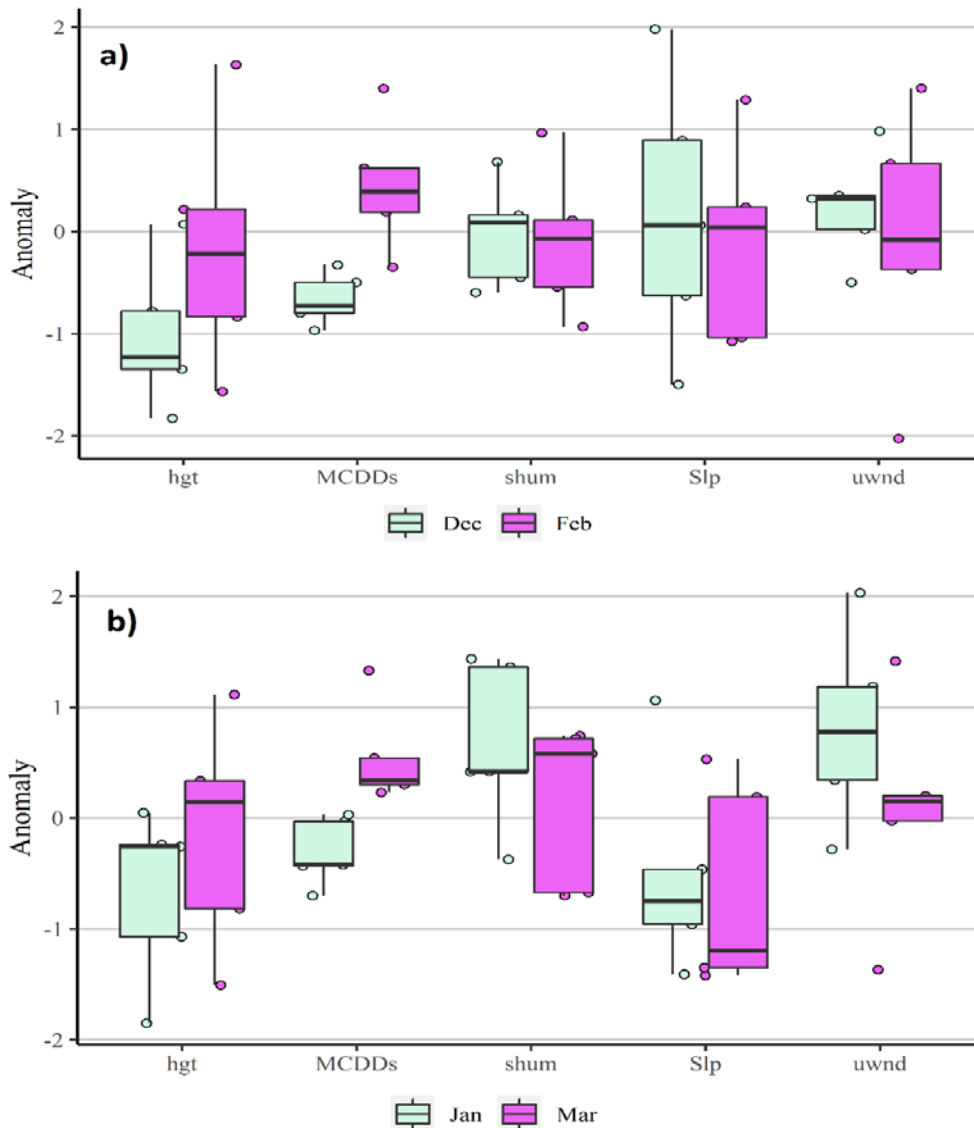


496 **Fig 8. Comparison of anomaly values (color shading) of large-scale atmospheric variables in LaNiña phases**  
 497 **between December (left panel) and January (right panel).**

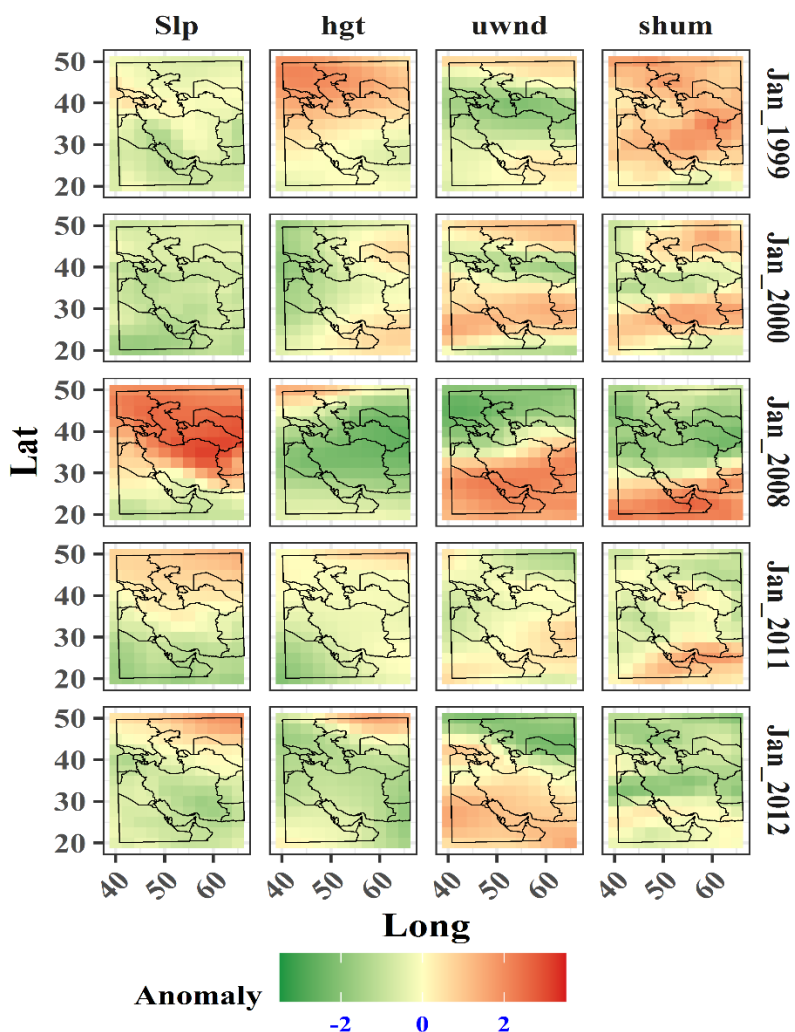
498 **Consistency analysis in anomalous values**

499 In the previous section, anomalous values for the El Niño and La Niña years were examined as  
 500 averages of 5 events occurring in different years (see Table 1). However, it is important to check  
 501 the consistency of the anomalous values for each of the 5 El Niño and La Niña years. As shown in  
 502 Table 5, in the El Niño years, the greatest differences in MCDDs anomaly values are observed  
 503 between December (negative) and February (positive) in the southwest. Fig 9 shows the boxplots  
 504 of MCDDs anomaly values and atmospheric variables during the La Niña and El Niño years.  
 505 During the El Niño years of December (Fig 9a. green color boxes), there is consistency in the  
 506 anomaly values of the MCDDs, the hgt-500, as well as the zonal wind in southwestern Iran. In  
 507 particular, there are negative and positive anomalies in the hgt-500 and the zonal wind,  
 508 respectively. In February during the El Niño years (Fig 9a. violet color boxes), there is consistency  
 509 in the MCDDs anomalies (apart from 2003 when the MCDDs anomaly is negative and the whole  
 510 situation is more similar to Dec 2002). The average MCDDs anomaly in the southwest is higher  
 511 in comparison with other regions, but it is not very high (0.47). However, the largest anomaly is  
 512 1.1 at latitude 31.5° and longitude 51.5. Although zonal wind anomalies and specific humidity are  
 513 mostly negative during the 5 El Niño events in the southwest, low consistency is observed among  
 514 the atmospheric variables. As mentioned before, in the La Niña years, the greatest difference  
 515 between January and March is observed in the southeast and this is why we present results for this  
 516 region in Fig. 9. In January (Fig 9b. green color boxes), in all La Niña years, the average MCDDs

517 anomaly is negative and the anomalies of the atmospheric variables are consistent with that. In  
 518 four out of five La Niña years, the values of SLP and hgt-500 have negative anomalies, while the  
 519 values of zonal wind and humidity have positive anomalies. Fig. 10 shows the anomalous values  
 520 of atmospheric variables during January for each of the La Niña years separately. All atmospheric  
 521 variables confirm that the MCDDs length decreases during La Niña in January in the southeastern  
 522 region. Finally, in March, during La Niña years (Fig 9b. violet color boxes), there are consistently  
 523 positive anomalies of MCDDs in the southeast. However, no stability can be observed in  
 524 atmospheric variables.



525 **Fig 9-** Boxplots of MCDDs and atmospheric variables anomalies during the La Niña and El Niño years a) in  
 526 December during El Niño years at southwest (green color boxes) and in February during El Niño years at  
 527 southwest (violet color boxes). b) in January during La Niña years at southeast (green color boxes) and in  
 528 March during La Niña years at southeast (violet color boxes). Dots represent the 5 strongest El Niño and La  
 529 Niña years (see Table 1).



531  
532 **Fig 10. The anomalous values of atmospheric variables during January in each of the La Niña years separately**  
533

534 Table 8 shows the correlation coefficients between the MCDDs with the ENSO index and the  
535 large-scale atmospheric variables for two points with the largest difference between MCDDs  
536 anomalies in the El Niño and La Niña phases in December (at latitude  $28.5^\circ$  and longitude 52.5)  
537 and January (at latitude  $28.5^\circ$  and longitude 54.5). Both grid points are located in the southwestern  
538 region. In January, the MCDDs anomaly during El Niño and La Niña phases is 0.3 and -1.36,  
539 respectively, at latitude  $28.5^\circ$  and longitude 54.5. The correlation coefficient between SLP and  
540 MCDDs is positive but statistically insignificant ( $R=0.3$ ) at both selected points (Table 8). This is  
541 consistent with the results of previous studies. Mariotti (2007) showed that in the relationship  
542 between southwest central Asia rainfall and ENSO the role of SLP is insignificant. Instead, the  
543 moisture flux plays a more important role. As presented in Table 6, in January, during El Niño (La  
544 Niña) years, a positive (negative) anomaly is observed in SLP and hgt and vice versa, a negative  
545 (positive) anomaly in zonal wind and specific humidity. The MCDDs have a positive and

546 statistically significant correlation with 850 and hgt-500. On the other hand, the correlations  
 547 between MCDDs and zonal and meridional winds, as well as humidity, are negative. A similar  
 548 relationship is seen between the ENSO index and the atmospheric parameters. For example, during  
 549 the positive phases, the zonal winds and the humidity are decreased. In December, the MCDDs  
 550 anomaly in El Niño and La Niña phases is -1.1 and 1.03, respectively, at latitude 28.5° and  
 551 longitude 52.5. During El Niño (La Niña) years, a negative (positive) anomaly is observed in 850  
 552 and 500- hpa hgt and vice versa, a positive (negative) anomaly in zonal wind and specific humidity.  
 553 Therefore, the situation in December is quite the opposite of that in January. The correlations  
 554 between the MCDDs and the ENSO index and large-scale atmospheric variables are similar to the  
 555 previously described grid point, but there is no significant correlation between MCDDs and SLP.

556 Nevertheless, the important point is that the relationship between ENSO and the 500-hpa hgt, 500-  
 557 hpa zonal winds and humidity in December is quite the opposite of that in January. In January, the  
 558 correlation coefficient between the ENSO and the 500-hpa specific humidity is negative and  
 559 statistically significant (-0.69), while in December it is positive and significant as well (0.71, see  
 560 Table 7). Fig. 11 shows three-dimensional scatter plots between atmospheric parameters (such as  
 561 SLP, hgt-500, zonal winds and specific humidity), MCDDs and the ENSO index. In December, at  
 562 latitude 28.5° and longitude 52.5 (shown with red colour in Figure 11), the relationship between  
 563 ENSO, zonal winds and humidity is positive. On the contrary, during January at latitude 28.5° and  
 564 longitude 54.5 (blue colour in Figure 11), ENSO has a negative relationship with those variables.  
 565 Therefore, this indicates that the ENSO index does not have the same effect in January and  
 566 December, proving the previously described non-stationary behavior.

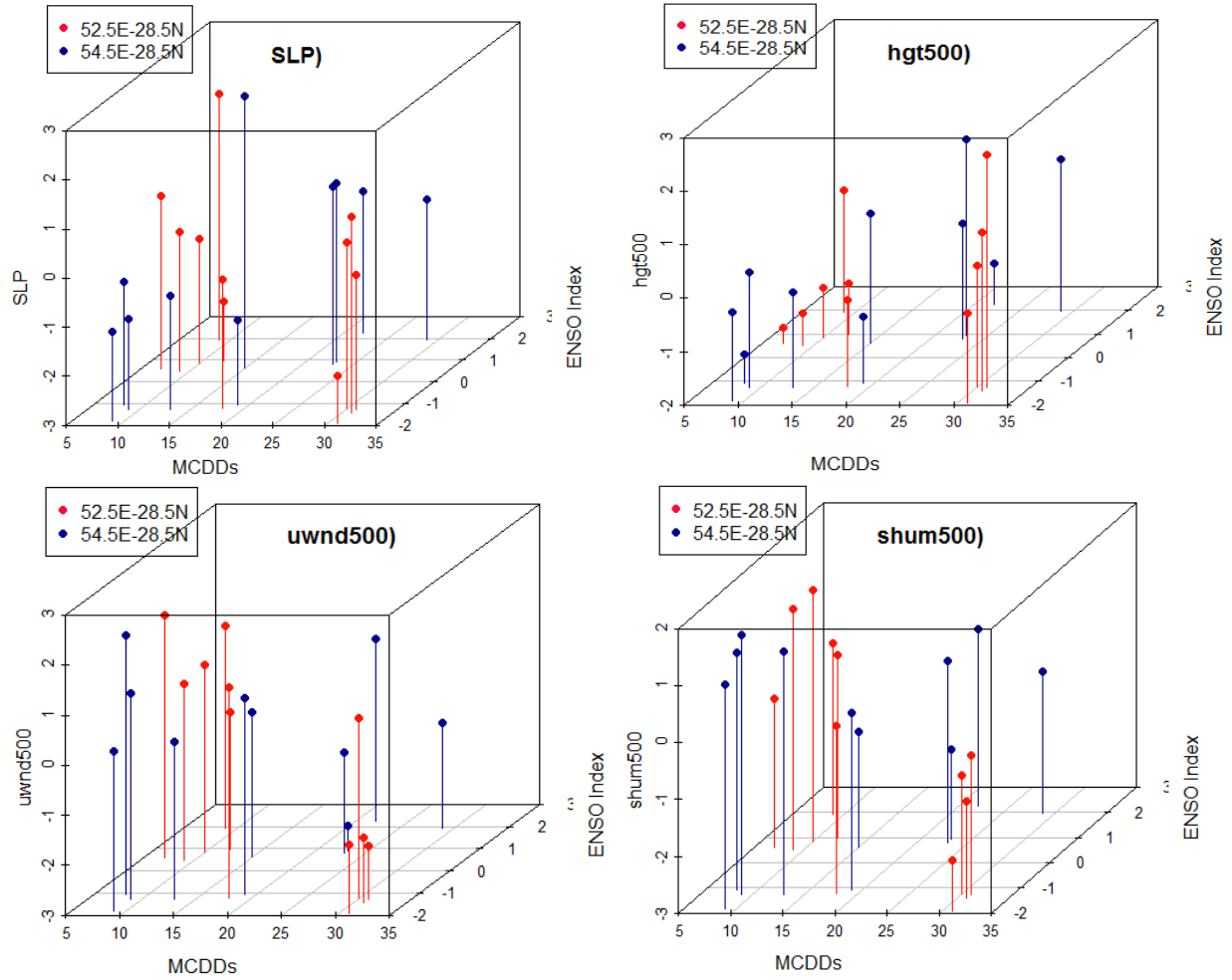
567 **Table 8- The comparison of correlation coefficients between ENSO and MCDDs with large-scale atmospheric**  
 568 **variables and anomaly values in two grid points in January and December.**

location	comparison		SLP	Hgt		vwnd		uwnd		shum		
				850hpa	500 hpa	850hpa	500 hpa	850hpa	500 hpa	850hpa	500 hpa	
54.5E_28.5N (Jan)	Anomaly	El Niño	0.74	0.79	0.4	-0.46	0.57	-0.64	-0.77	-0.34	-0.51	
		La Niña	-0.95	-1.07	-0.51	0.67	0.19	0.45	0.91	0.9	1.01	
	Cor	MCDDs vs.	0.3	0.48*	0.45*	-0.64**	-0.03	-0.1	-	0.67**	-0.69**	-0.7**
		ENSO vs.	0.55**	0.55**	0.31	-0.47*	0.21	-0.23	-0.5**	-0.56**	-	0.69**
52.5E_28.5N (Dec)	Anomaly	El Niño	0.02	-0.87	-0.98	0.5	0.77	0.3	0.78	0.61	0.5	
		La Niña	-0.25	0.3	0.56	-0.34	-0.19	-0.79	-0.69	-0.84	-0.98	
	Cor	MCDDs vs.	-0.16	0.55**	0.74**	-0.63**	-0.40*	-0.74**	-	0.77**	-0.73**	-
		ENSO vs.	0.3	-0.31	-0.49*	0.44*	0.63**	0.53**	0.59**	0.7**	0.71**	

\*\* Significant at level of p=0.01

\* Significant at the level of p=0.05

569  
570



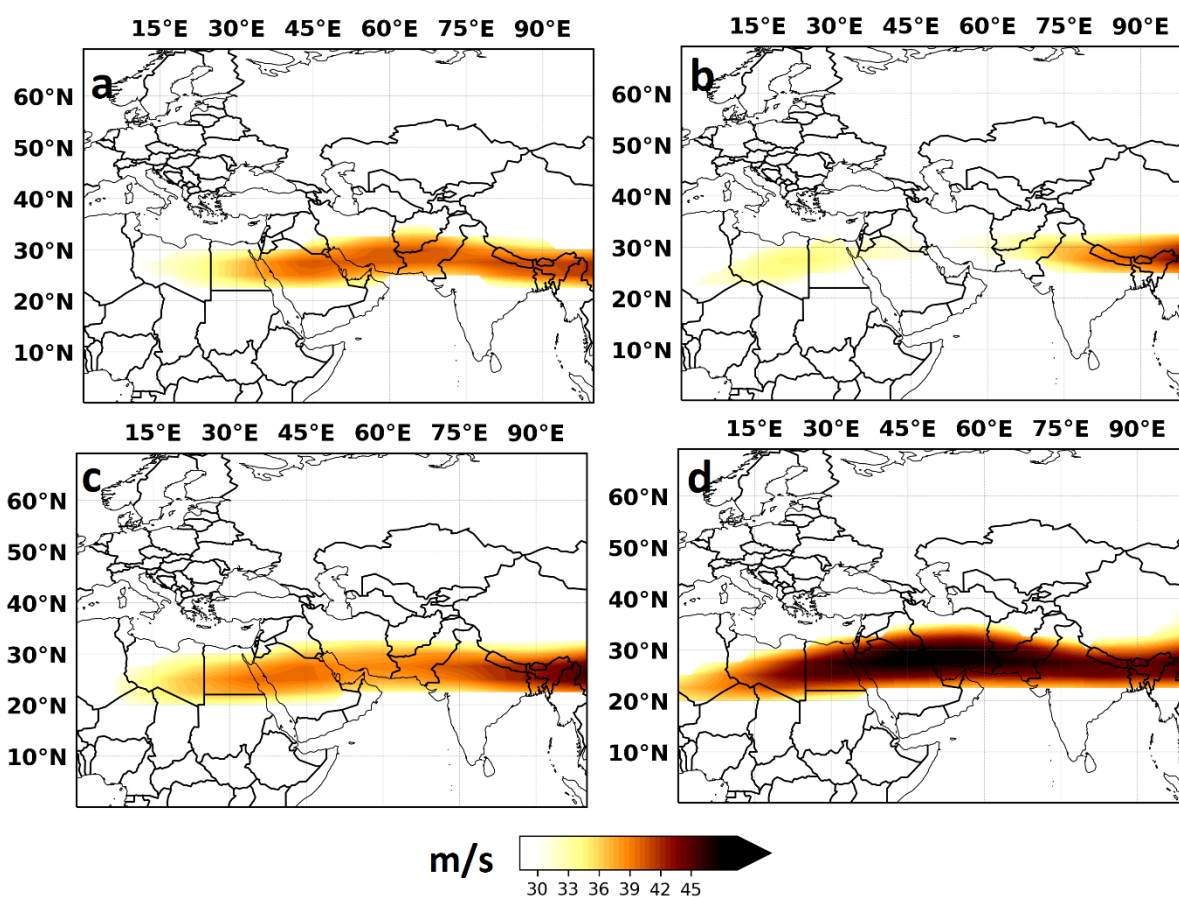
571  
 572  
 573  
 574  
 575  
 576  
 577  
 578  
 579  
 580  
 581  
 582  
 583  
 584  
 585  
 586  
 587  
 588  
 589  
 590

**Fig. 11. Three-dimensional scatter plots of ENSO, MCDDs, and atmospheric variables in the two points in January (54.5E\_28.5N, blue colour) and December (52.5E\_28.5N, red colour) in El Niño and La Niña phases.**



591 **Jet stream pattern**

592 Precipitation anomalies are related with changes in the jet stream position (Belmecheri et al. 2017;  
593 Gaetani et al., 2011). Fig. 12 compares the jet stream patterns in the El Niño and La Niña years  
594 between January and December. In January, jet stream values are weaker in the El Niño years (Fig.  
595 12 c) compared to the La Niña years (Fig. 12 d) over Iran, and especially in the southern half of  
596 the country, where during La Niña the wind speeds exceed 45 m/s in this region. This is consistent  
597 with the results in the previous section that in the La Niña-January period the length of MCDDs is  
598 shorter in southeastern Iran (compared to El Niño periods). On the other hand, the jet stream pattern  
599 in December is completely opposite to that of January. In the El Niño periods (Fig. 12 a), wind  
600 speeds in the southern half are stronger than in the La Niña periods (Fig. 12 b). For this reason, in  
601 December, the MCDDs length is shorter during El Niño and especially in the southwest part of the  
602 country.



603  
604 **Fig 12. Comparison of jetstream patterns at 300-hPa in the El Niño and La Niña years. a) December - El Niño**  
605 **years. b) December – La Niña years. c) January - El Niño years. d) January – La Niña years.**

606  
607 **Discussion and Conclusions**

608 In this study, the characteristics of the Maximum Number of Consecutive Dry Days (MCDDs)  
609 were investigated using satellite data (TRMM- 3B42RT) for 1998-2019 on a daily basis in Iran.  
610 The major results obtained in this study are as follows:

611 1) The highest and lowest MCDDs values were observed in southeastern and northwestern Iran,  
612 respectively. The maximum and minimum spatial monthly average of MCDDs were observed  
613 during Dec ( $15.8 \pm 6.4$ ) and Feb ( $12.8 \pm 5.2$ ), respectively.

614 2) The analysis of the linear trends of the MCDDs indicated mostly positive coefficients in Iran.  
615 A significant increasing trend was observed in the MCDDs in all months and over the largest part  
616 of the country. However, a declining trend is dominant in some places in the southeastern region.  
617 The number of points with a significant trend of the MCDDs was more abundant in January and  
618 December. Also, spatially the highest number of points with a significant trend in the MCDDs was  
619 observed in northwestern and southeastern Iran.

620 3) The results of the correlation analysis between MCDDs and ENSO indicated that the effect of  
621 ENSO varies from month to month. In December and March, the relationship between MCDDs  
622 and ENSO is negative, but in January and February, the relationship is positive. Therefore, in the  
623 El Niño phases, the length of MCDDs increased in January (in the eastern half) and February  
624 (especially in the southwest), but decreased in December (especially in the southern half). These  
625 conditions are reversed in the La Niña phases. The analysis of the ENSO effect mechanism on  
626 MCDDs length showed that in each phase of El Niño and La Niña, there was a significant  
627 difference in the values of hgt-500, zonal wind, specific humidity and jet stream pattern between  
628 December and January, which explains why the effect on dry spells differs from one winter month  
629 to another. In particular, during El Niño (La Niña) phases, a negative (positive) anomaly of the  
630 geopotential height, and a positive (negative) anomaly of the zonal wind component and of the  
631 specific humidity were observed in December (January). This causes the length of MCDDs to  
632 increase (decrease) especially in the southern half in January (December) during the warm ENSO  
633 phases.

634 As seen in the results of this study, the largest differences between December and January seen in  
635 the effect of La Niña on dry spells over Iran, can be explained by the pronounced differences in  
636 the location and strength of the jet stream between the two months. In January the subtropical jet  
637 stream appears much more pronounced and located over the southern part of Iran, while in  
638 December the winds are very weak over the whole country. The reason why the jet stream response  
639 to La Niña is so different between December and January is a question that remains open and  
640 requires further dynamical analysis. Concluding, as Iran lies in a region that is not always directly  
641 affected by ENSO conditions, it seems that there are other dynamical processes in play that define  
642 the response of dry spells ~~even~~ more than ENSO, or that the response to ENSO is asynchronous  
643 and not simultaneous, as supported by Mohammadrezaei et al. (2020).

644 Therefore, based on satellite data that provide us with continuous spatial coverage over Iran, we  
645 find that El Niño (La Niña) has contradictory, non-stationary effects on MCDDs in different winter  
646 months, whereas previous studies have only referred to the positive (negative) effect of El Niño  
647 (La Niña) on Iranian rainfall in the autumn season. Hence, our findings can be useful in planning  
648 with regards to soil moisture, streamflow, groundwater and rainfed agriculture and thus of great  
649 importance for decision makers and stakeholders in Iran.

650 **-Conflict of Interest:**  
651 The authors declare that there are no conflicts of interest regarding the publication of this paper.

652  
653 **-Funding Statement:**  
654 The authors declare that there was no funding for the present study.

655  
656 **-Author's Contribution:**  
657 Mohammad Rezaei presented the initial idea of the work and supervised the study together with Efi Rousi.  
658 Elham. Gh and Ali S. helped in statistical analysis. The final version is written by Mohammad Rezaei and  
659 revised by Efi Rousi. The order of the authors is based on the level of their contribution.

660  
661 **-Availability of data and material:**  
662 The data that support the findings of this study are available from the corresponding author, upon reasonable  
663 request.

664  
665 **-Code availability:**  
666 The codes that support the findings of this study are available from the corresponding author.

667 **-Ethics approval:**  
668 The authors declare that there is no human or animal participant in the study. Not applicable

669  
670 **-Consent to participate:**  
671 The authors declare that there is no human or animal participant in the study. Not applicable

672  
673 **-Consent for publication:**  
674 The authors give their consent to publication of all detailed of the manuscript including texts, figures and  
675 tables.

676  
677 **References**

- 678  
679 1. Abarghouei, H. B., Zarch, M. A. A., Dastorani, M. T., Kousari, M. R., &Zarch, M. S (2011) The survey of  
680 climatic drought trend in Iran. *Stochastic Environmental Research and Risk Assessment*, 25(6), 851.  
681 2. Ahmadi, M., Salimi, S., Hosseini, S. A., Poorantiyosh, H., &Bayat, A (2019) Iran's precipitation analysis  
682 using synoptic modeling of major teleconnection forces (MTF). *Dynamics of Atmospheres and Oceans*, 85,  
683 41-56.  
684 3. Alijani, B (2002) Variations of 500 hPa flow patterns over Iranand surrounding areas and their relationship  
685 with the climate of Iran. *Theoretical and applied climatology*, 72(1-2), 41-54.  
686 4. Alizadeh-Choobari, O., Adibi, P., &Irannejad, P (2018) Impact of the El Niño–Southern Oscillation on the  
687 climate of Iran using ERA-Interim data. *Climate dynamics*, 51(7-8), 2897-2911.  
688 5. Anagnostopoulou C, Maheras P, Karacostas T, Vafiadis M (2003) Spatial and temporal analysis of dry spells  
689 in Greece. *TheorApplClimatol* 74:77–91.

- 690 6. Araghi, A., Mousavi-Baygi, M., Adamowski, J., & Martinez, C (2017) Association between three prominent  
691 climatic teleconnections and precipitation in Iran using wavelet coherence. *International Journal of*  
692 *Climatology*, 37(6), 2809-2830.
- 693 7. Asakereh, H (2017) Trends in monthly precipitation over the northwest of Iran (NWI). *Theoretical and*  
694 *Applied Climatology*, 130(1-2), 443-451.
- 695 8. Ashraf, B., Yazdani, R., Mousavi-Baygi, M., & Bannayan, M (2014) Investigation of temporal and spatial  
696 climate variability and aridity of Iran. *Theoretical and Applied Climatology*, 118(1-2), 35-46.
- 697 9. Barrucand, M. G., Vargas, W. M., & Rusticucci, M. M (2007) Dry conditions over Argentina and the related  
698 monthly circulation patterns. *Meteorology and Atmospheric Physics*, 98(1-2), 99-114.
- 699 10. Bazrafshan, J., & Khalili, A (2013) Spatial Analysis of Meteorological Drought in Iran from 1965 to 2003.  
700 *Desert*, 18(1), 63-71.
- 701 11. Belmecheri, S., Babst, F., Hudson, A. R., Betancourt, J., & Trouet, V (2017) Northern Hemisphere jet stream  
702 position indices as diagnostic tools for climate and ecosystem dynamics. *Earth Interactions*, 21(8), 1-23.
- 703 12. Biabanaki, M., Eslamian, S. S., Koupai, J. A., Cañón, J., Boni, G., & Gheysari, M (2014) A principal  
704 components/singular spectrum analysis approach to ENSO and PDO influences on rainfall in western Iran.  
705 *Hydrology Research*, 45(2), 250-262.
- 706 13. Brocca, L., Massari, C., Pellarin, T., Filippucci, P., Ciabatta, L., Camici, S., ... & Fernández-Prieto, D (2020)  
707 River flow prediction in data scarce regions: soil moisture integrated satellite rainfall products outperform  
708 rain gauge observations in West Africa. *Scientific Reports*, 10(1), 1-14.
- 709 14. Bonsal, B. R., & Lawford, R. G (1999) Teleconnections between El Niño and La Niña events and summer  
710 extended dry spells on the Canadian Prairies. *International Journal of Climatology: A Journal of the Royal*  
711 *Meteorological Society*, 19(13), 1445-1458.
- 712 15. Caloiero, T., Coscarelli, R., Ferrari, E., & Sirangelo, B (2015) Analysis of dry spells in southern Italy  
713 (Calabria). *Water*, 7(6), 3009-3023.
- 714 16. Cindrić, K., Pasarić, Z., & Gajić-Čapka, M (2010) Spatial and temporal analysis of dry spells in Croatia.  
715 *Theoretical and applied climatology*, 102(1-2), 171-184
- 716 17. Darand, M., Amanollahi, J., & Zandkarimi, S (2017) Evaluation of the performance of TRMM Multi-satellite  
717 Precipitation Analysis (TMPA) estimation over Iran. *Atmospheric Research*, 190, 121-127.
- 718 18. Dehghani, M., Salehi, S., Mosavi, A., Nabipour, N., Shamshirband, S., & Ghamisi, P (2020) Spatial Analysis  
719 of Seasonal Precipitation over Iran: Co-Variation with Climate Indices.
- 720 19. Deni, S. M., Suhaila, J., Zin, W. Z. W., & Jemain, A. A (2010) Spatial trends of dry spells over Peninsular  
721 Malaysia during monsoon seasons. *Theoretical and applied climatology*, 99(3-4), 357.
- 722 20. Dezfuli, A. K., Karamouz, M., & Araghinejad, S (2010) On the relationship of regional meteorological  
723 drought with SOI and NAO over southwest Iran. *Theoretical and applied climatology*, 100(1-2), 57-66.
- 724 21. Domroes, M., Kaviani, M., & Schaefer, D (1998) An analysis of regional and intra-annual precipitation  
725 variability over Iran using multivariate statistical methods. *Theoretical and Applied Climatology*, 61(3-4),  
726 151-159.

- 727 22. Douguedroit, A (1987) The variations of dry spells in Marseilles from 1865 to 1984. *Journal of Climatology*,  
728 7(6), 541-551.
- 729 23. Duan, Y., Ma, Z., & Yang, Q (2017) Characteristics of consecutive dry days variations in China. *Theoretical*  
730 *and Applied Climatology*, 130(1-2), 701-709.
- 731 24. Gaetani, M., Baldi, M., Dalu, G. A., Maracchi, G., Lionello, P., & Trigo, R (2011) Jetstream and rainfall  
732 distribution in the Mediterranean region. *Natural Hazards & Earth System Sciences*, 11(9).
- 733 25. Golian, S., Mazdiyasi, O., & AghaKouchak, A (2015) Trends in meteorological and agricultural droughts in  
734 Iran. *Theoretical and applied climatology*, 119(3-4), 679-688.
- 735 26. Griffith, D. A (2003) *Spatial autocorrelation and spatial filtering: gaining understanding through theory and*  
736 *scientific visualization*. Springer Science & Business Media.
- 737 27. Hosseinzadeh, S (2004) Environmental crises in the metropolises of Iran. *WIT Trans. Ecol. Environ.* 72.
- 738 28. Hosseinzadeh Talaee, P., Tabari, H., & Sobhan Ardakani, S (2014) Hydrological drought in the west of Iran  
739 and possible association with large-scale atmospheric circulation patterns. *Hydrological Processes*, 28(3),  
740 764-773.
- 741 29. IPCC (2007) *Climate change: synthesis report of the fourth assessment report*. IPCC, Geneva
- 742 30. Lana X, Martinez MD, Burgueno A, Serra C, Martin-Vide J, Gomez L (2008) Spatial and temporal patterns  
743 of dry spell lengths in the Iberian Peninsula for the second half of the twentieth century. *TheorApplClimatol*  
744 91:99–116
- 745 31. Llano, M. P., & Penalba, O. C (2011) A climatic analysis of dry sequences in Argentina. *International journal*  
746 *of climatology*, 31(4), 504-513
- 747 32. Kalnay, E., Kanamitsu, M., Kistler, R., Collins, W., Deaven, D., Gandin, L., ... & Zhu, Y (1996) The  
748 NCEP/NCAR 40-year reanalysis project. *Bulletin of the American meteorological Society*, 77(3), 437-472.
- 749 33. Kutiel H (1985) The multimodality of the rainfall course in Israel as reflected by the distribution of dry spells.  
750 *ArchMetGeophBioclimSer B39*: 15–27
- 751 34. Kutiel H, Maheras P (1992) Variations Interannuelles des s\_equencess\_echeset des situations  
752 synoptiquesenM\_editerrann\_ee. *Publications de l'AIC 5*: 15–27
- 753 35. Mariotti, A (2007) How ENSO impacts precipitation in southwest central Asia. *Geophysical Research*  
754 *Letters*, 34(16).
- 755 36. Martin-Vide J, Gomez L (1999) Regionalization of peninsular Spain based on the length of dry spells. *Int J*  
756 *Climatol* 19:537–555
- 757 37. McCabe, G. J., Legates, D. R., & Lins, H. F (2010) Variability and trends in dry day frequency and dry event  
758 length in the southwestern United States. *Journal of Geophysical Research: Atmospheres*, 115(D7).
- 759 38. Min, S. K., Zhang, X., Zwiers, F. W., & Hegerl, G. C (2011) Human contribution to more-intense  
760 precipitation extremes. *Nature*, 470(7334), 378-381.
- 761 39. Mohammadrezaei, M., Soltani, S., & Modarres, R (2020) Evaluating the effect of ocean-atmospheric indices  
762 on drought in Iran. *Theoretical and Applied Climatology*, 140(1), 219-230.
- 763 40. Modarres, R (2006) Regional precipitation climates of Iran. *J. Hydrol. (N. Z.)* 13–27.

- 764 41. Modarres, R., & Sarhadi, A (2009) Rainfall trends analysis of Iran in the last half of the twentieth century.  
765 Journal of Geophysical Research: Atmospheres, 114(D3).
- 766 42. Moran, P. A (1950) Notes on continuous stochastic phenomena. *Biometrika*, 37(1/2), 17-23.
- 767 43. Najafi, M. R., & Moazami, S (2016) Trends in total precipitation and magnitude–frequency of extreme  
768 precipitation in Iran, 1969–2009. *International Journal of Climatology*, 36(4), 1863-1872.
- 769 44. Nasri, M., & Modarres, R (2009) Dry spell trend analysis of Isfahan Province, Iran. *International Journal of*  
770 *Climatology: A Journal of the Royal Meteorological Society*, 29(10), 1430-1438.
- 771 45. Nazaripour, H., & Daneshvar, M. M (2014) Spatial contribution of one-day precipitations variability to rainy  
772 days and rainfall amounts in Iran. *International Journal of Environmental Science and Technology*, 11(6),  
773 1751-1758.
- 774 46. Nazemosadat, M. J., & Cordery, I (2000,a) On the relationships between ENSO and autumn rainfall in Iran.  
775 *International Journal of Climatology: A Journal of the Royal Meteorological Society*, 20(1), 47-61.
- 776 47. Nazemosadat, M. J., & Cordery, I (2000,b) The impact of ENSO on winter rainfall in Iran. *Hydro 2000:*  
777 *Interactive Hydrology; Proceedings*, 538.
- 778 48. Newman, M., Compo, G. P., & Alexander, M. A (2003) ENSO-forced variability of the Pacific decadal  
779 oscillation. *Journal of Climate*, 16(23), 3853-3857.
- 780 49. Oikonomou, C., Flocas, H. A., Hatzaki, M., Nisantzi, A., & Asimakopoulos, D. N (2010) Relationship of  
781 extreme dry spells in Eastern Mediterranean with large-scale circulation. *Theoretical and applied*  
782 *climatology*, 100(1-2), 137-151.
- 783 50. Raymond, F., Ullmann, A., Camberlin, P., Oueslati, B., & Drobinski, P (2018) Atmospheric conditions and  
784 weather regimes associated with extreme winter dry spells over the Mediterranean basin. *Climate Dynamics*,  
785 50(11-12), 4437-4453.
- 786 51. Razieli, T., Mofidi, A., Santos, J. A., & Bordi, I (2012) Spatial patterns and regimes of daily precipitation in  
787 Iran in relation to large-scale atmospheric circulation. *International Journal of Climatology*, 32(8), 1226-  
788 1237.
- 789 52. Razieli, T., Daryabari, J., Bordi, I., & Pereira, L. S (2014) Spatial patterns and temporal trends of precipitation  
790 in Iran. *Theoretical and applied climatology*, 115(3-4), 531-540.
- 791 53. Schmidli, J., & Frei, C (2005) Trends of heavy precipitation and wet and dry spells in Switzerland during the  
792 20th century. *International Journal of Climatology: A Journal of the Royal Meteorological Society*, 25(6),  
793 753-771.
- 794 54. Sang, Y. W., Yik, D. J., Chang, N. K., & Yunus, F (2015) Analysis on the Long Term Trends of Consecutive  
795 Dry and Wet Days and Extreme Rainfall Amounts in Malaysia. Malaysian Meteorological Department.
- 796 55. Seleshi, Y., & Camberlin, P (2006) Recent changes in dry spell and extreme rainfall events in Ethiopia.  
797 *Theoretical and Applied Climatology*, 83(1-4), 181-191
- 798 56. Serra C, Burgueno A, Martinez MD, Lana X (2006) Trends in dry spells across Catalonia (NE Spain) during  
799 the second half of the 20th century. *TheorApplClimatol* 85:165–183

- 800 57. Sezen, C., &Partal, T (2019) The impacts of Arctic oscillation and the North Sea Caspian pattern on the  
801 temperature and precipitation regime in Turkey. *Meteorology and Atmospheric Physics*, 131(6), 1677-1696.
- 802 58. Shenbrot, G.I., Krasnov, B.R., Rogovin, K.A (1999) Deserts of the world. In: *Spatial Ecology of Desert*  
803 *Rodent Communities*. Springer, pp. 5–24.
- 804 59. Singh, N., &Ranade, A (2010) The wet and dry spells across India during 1951–2007. *Journal of*  
805 *Hydrometeorology*, 11(1), 26-45
- 806 60. Sivakumar MVK (1992) Empirical analysis of dry spells for agricultural applications in west Africa. *J Clim*  
807 5:532–539
- 808 61. Some'e, B. S., Ezani, A., &Tabari, H (2012) Spatiotemporal trends and change point of precipitation in Iran.  
809 *Atmospheric research*, 113, 1-12.
- 810 62. Suppiah, R., & Hennessy, K. J (1998) Trends in total rainfall, heavy rain events and number of dry days in  
811 Australia, 1910–1990. *International Journal of Climatology: A Journal of the Royal Meteorological Society*,  
812 18(10), 1141-1164.
- 813 63. Tabari, H., &Talaee, P. H (2011) Temporal variability of precipitation over Iran: 1966–2005. *Journal of*  
814 *Hydrology*, 396(3-4), 313-320
- 815 64. Unal, Y. S., Deniz, A., Toros, H., &Incecik, S (2012) Temporal and spatial patterns of precipitation variability  
816 for annual, wet, and dry seasons in Turkey. *International Journal of Climatology*, 32(3), 392-405.
- 817 65. Wang, H., Chen, Y., Pan, Y., & Li, W (2015) Spatial and temporal variability of drought in the arid region  
818 of China and its relationships to teleconnection indices. *Journal of hydrology*, 523, 283-296.
- 819 66. Zhang, X., Zwiers, F. W., Hegerl, G. C., Lambert, F. H., Gillett, N. P., Solomon, S., ... &Nozawa, T (2007)  
820 Detection of human influence on twentieth-century precipitation trends. *Nature*, 448(7152), 461-465.
- 821